THE COLLEGE OF AERONAUTICS

CRANFIELD

THE DESIGN OF MICHELL OPTIMUM STRUCTURES

by

A. S. L. CHAN

THE COLLEGE OF AERONAUTICS

CRANFIELD

The Design of Michell Optimum Structures

- by -

A. S. L. Chan, B.Sc., M.Sc.,
D.I.C., A.F.R.Ae.S.

SUMMARY

The fundamental problem of structural design is the determination
of structures of minimum weight which safely equilibrate a given
system of external forces. The classical theorem of Michell gave the
basic requirements for such a structure. The first part of this paper
analyses the geometrical layout of two-dimensional structures which
satisfy these requirements, making use of the analogy with the theory
of plane plastic flow. Expressions for the calculation of sizes and the
total volume of the structural members are developed. Method of
graphical construction of the structural layout is also given.

In the second part, the analogy with a known solution of plastic
flow is used to develop solutions for a cantilever under tip shear
force and a beam under uniform bending moment. Comparisons with
the conventional types of construction are made and the superiority
of the Michell structures are demonstrated.

CONTENTS

Contents (Continued)

NOTATION

A, B	Lame's Parameters, defined in eq. (1)
a, b	+1 or -1 (eq. 11)
C	compressive forces in members
d	depth of cantilever or beam at the supports
e	strain
f	stress
F	external applied forces
G	Green's function, defined in eq. (26)
I	Modified Bessel Functions
J	Bessel Functions
ℓ	span of cantilever or beam
M	external applied moment
r	radius of circular arcs
s	distance along any line
t_1, t_2	equivalent thicknesses of sheets of elements
T_1, T_2	$= t_1 B$ and $t_2 A$ respectively as defined in eq. (32)
T	tensile forces in members
u, v	virtual displacements in α, β directions
V	volume of structure
x, y	rectangular co-ordinates
α, β	curvilinear co-ordinates
ϕ	angle between α-direction and x-direction
σ, τ	another set of variables defined in eq. (57)
ω	rotation

Other symbols are defined in the text.

PART I

MICHELL OPTIMUM STRUCTURES

1. Introduction

The basic problem of structural design, as opposed to structural analysis, is the determination of structures of minimum weight, which equilibrate, with safety, a given system of external forces. The classical theorem in this subject is due to Michell (Ref. 1). Recent interest in Michell structures has stemmed from two sources. Cox (Ref. 2,3) and Hemp (Ref. 4) have considered the application of Michell's results to 'elastic' design problems, while Drucker and Shield (Ref. 5) and Prager (Ref. 6) have developed and applied the corresponding results in the field of 'limit design'. These two problems are closely related mathematically and owe much to the techniques developed in the field of perfect plastic flow, accounts of which are given by, for example, Geiringer (Ref. 7), Hill (Ref. 8) and Prager (Ref. 9). The present paper makes much use of this analogy.

2. Michell's Theorem

Consider the problem of designing a frame structure S, within a given region of space R, to equilibrate a given system of forces or to transmit their action to given surfaces of rigid support. Let us assume that there exists such a framework S^* which satisfies the following conditions:

(1) The stresses in all members are equal to $\pm f$, where f is the 'allowable stress' for tension and compression.

(2) There exists a virtual deformation of the region R, with displacement vanishing on the surfaces of support and with strains along the members of S^* equal to $\pm e$, where the sign agrees with that of the end load carried by the particular member, and such that no linear strain in R exceeds e, which is a small positive number, in absolute value.

Michell's Theorem then states that the volume of the structure S^* is less than or equal to that of any other frame work S, which safely equilibrates the given forces. Proofs of this result are to be found in Refs. 1 and 4.

One immediate consequence may be noted. If in a particular problem it is found possible to design a structure all of whose members are in tension, or alternatively compression, then the optimum design

has been achieved, since a uniform dilatation of space with linear strain e, or alternatively (-e), clearly satisfies condition (2) above. This special case will not be considered any further in this paper.

In general it is clear that the members of the optimum structure S^* must lie along lines of principal strain in the virtual deformation, since, if this were not so, a direction could be found, at a point on a member, for which the direct strain had a magnitude greater than e, contrary to condition (2). Also a tension and compression member, which meet at a node, must be orthogonal, since they lie along principal directions with unequal principal strains e and (-e). The layout lines for members of S^* are thus lines of principal strain in a strain field whose principal strains are $\pm$ e. A study of this kind of strain field is thus a necessary pre-requisite for the construction of Michell optimum frame works.

3. Analysis of the Virtual Deformation

Attention will be confined, for simplicity, to the special case of two-dimensional frameworks and those corresponding deformation patterns for which the principal strains are e and (-e). The lines of principal strain then form a plane net of orthogonal curves, which may be used to define, in at least a limited region of the plane, a right-handed curvilinear co-ordinate system (α, β) for which the line element ds is given by

$$ds^2 = A^2 d\alpha^2 + B^2 d\beta^2 \tag{1}$$

where A, B are positive functions of α, β. Positive directions along the co-ordinate curves are taken as those for which α and β are increasing and at any point in the plane these directions may be used to define components of virtual displacement (u, v) (see Fig. 1). The direct strain in the α-direction will be taken as (e) and that in the β-direction as (-e). The associated shear strain is zero, since these directions are principal directions. Finally the rotation at (α, β) will be denoted by ω.

The relations between the displacement components and the strains and rotation are given for curvilinear co-ordinates by Love (Ref. 10). Using these results one obtains the equations:

$$\frac{1}{A} \frac{\partial u}{\partial \alpha} + \frac{v}{AB} \frac{\partial A}{\partial \beta} = e , \tag{2}$$

$$\frac{1}{B} \frac{\partial v}{\partial \beta} + \frac{u}{AB} \frac{\partial B}{\partial \alpha} = -e , \tag{3}$$

$$\frac{B}{A} \frac{\partial}{\partial \alpha}(\frac{v}{B}) + \frac{A}{B} \frac{\partial}{\partial \beta} (\frac{u}{A}) = 0 , \tag{4}$$

and $$\frac{1}{AB} \left[\frac{\partial}{\partial \alpha}(Bv) - \frac{\partial}{\partial \beta} (Au) \right] = 2\omega. \tag{5}$$

Further transformation is facilitated by the introduction of the angle ϕ between the positive α-direction and a fixed reference direction, which may be taken as the x-axis of a right-handed orthogonal Cartesian systems $O(x,y)$ (see Fig. 1). It may be shown as in Ref. 4, Appendix A that

$$\frac{\partial \phi}{\partial \alpha} = -\frac{1}{B} \frac{\partial A}{\partial \beta} , \qquad \frac{\partial \phi}{\partial \beta} = \frac{1}{A} \frac{\partial B}{\partial \alpha} . \tag{6}$$

Solving equations (2) ... (5) for the derivatives of u, v and eliminating the derivatives of A, B by (6) gives

$$\frac{\partial u}{\partial \alpha} = A e + v \frac{\partial \phi}{\partial \alpha} , \qquad \frac{\partial u}{\partial \beta} = - B\omega + v \frac{\partial \phi}{\partial \beta} , \tag{7}$$

$$\frac{\partial v}{\partial \alpha} = A \omega - u \frac{\partial \phi}{\partial \alpha} , \qquad \frac{\partial v}{\partial \beta} = - Be - u \frac{\partial \phi}{\partial \beta} . \tag{8}$$

Elimination of u, v between (7) and (8) gives

$$\frac{\partial}{\partial \alpha}(\omega - 2e \phi) = 0, \qquad \frac{\partial}{\partial \beta}(\omega + 2e \phi) = 0, \tag{9}$$

and elimination of ω gives

$$\frac{\partial^2 \phi}{\partial \alpha \partial \beta} = 0. \tag{10}$$

Equation (10) is the compatibility equation for the Michell virtual strain system. It expresses a geometrical restriction on the form of the layout lines, which is identical with that expressed by Hencky's Theorem for the slip-lines in plane plastic flow. The analogy with plastic flow is seen even more closely in equations (9), due to Prager (Ref. 6), which may be compared with the Hencky results as given for example in Hill (Ref. 8).

4. Introduction of Special Co-ordinate Systems

(A) Case 1.

Consider first of all the curves where $\frac{\partial \phi}{\partial \alpha}$ and $\frac{\partial \phi}{\partial \beta}$ do not vanish in the region of our co-ordinate system which is of interest to us. This means that in this region the co-ordinate curves have no inflexions. In this case it is convenient to choose the co-ordinates α, β as numerically equal to the values of ϕ on a fixed pair of co-ordinate curves (Fig. 2). Equation (10) then integrates as

$$\phi = a\alpha + b\beta \qquad (a, b = \pm 1), \tag{11}$$

(cf Ref. 7), and the various cases are illustrated in the diagrams (a) to (d) of Fig. 2. A formula for ω follows from (9), which gives

$$\omega = 2e (a\alpha - b\beta) + \omega_0, \tag{12}$$

where ω_0 is the value of ω when $\alpha = \beta = 0$. Equations for A, B follow from (6), giving

$$\frac{\partial A}{\partial \beta} = -aB, \qquad \frac{\partial B}{\partial \alpha} = bA, \tag{13}$$

and hence,

$$\left. \begin{aligned} \frac{\partial^2 A}{\partial \alpha \partial \beta} + abA &= 0, \\[2mm] \frac{\partial^2 B}{\partial \alpha \partial \beta} + abB &= 0. \end{aligned} \right\} \tag{14}$$

Finally, (7) and (8) give for u, v the equations

$$\left. \begin{aligned} \frac{\partial u}{\partial \alpha} - av &= Ae, & \frac{\partial u}{\partial \beta} - bv &= -B\omega, \\[2mm] \frac{\partial v}{\partial \alpha} + au &= A\omega, & \frac{\partial v}{\partial \beta} + bu &= -Be, \end{aligned} \right\} \tag{15}$$

which may be integrated, since ω is known by (12), as soon as A, B are determined.

(B) Case 2.

Consider next the case where $\frac{\partial \phi}{\partial \alpha}$ = 0 everywhere in the region under consideration. The α co-ordinate curves are then straight lines, which in general envelope an 'evolute'. The β-co-ordinate curves are then 'involutes' (Fig. 3). It is now convenient to choose α as the distance measured along the α-lines from a fixed involute (α = 0) and, in the case when the β-curves have no inflexions, to take β as the angle between the corresponding α-lines and a fixed α-line (β = 0), (see Fig. 3). We now have,

$$A = 1, \quad B = \alpha + F(\beta), \quad \phi = \beta , \tag{16}$$

where F(β) is the distance from α = 0 to the evolute and ϕ is measured from the line β = 0. Equations (9) give

$$\omega = -2e\beta + \omega_0 \tag{17}$$

and (7) and (8) simplify to

$$\left. \begin{array}{ll} \dfrac{\partial u}{\partial \alpha} = e , & \dfrac{\partial u}{\partial \beta} - v = -B\omega , \\[3mm] \dfrac{\partial v}{\partial \alpha} = \omega , & \dfrac{\partial v}{\partial \beta} + u = -Be , \end{array} \right\} \tag{18}$$

where B, ω are given by (16) and (17). These can be readily integrated when F(β) is known.

(C) Case 3.

Finally, when $\frac{\partial \phi}{\partial \alpha} = \frac{\partial \phi}{\partial \beta}$ = 0 we can take α, β as orthogonal Cartesian co-ordinates with

$$A = B = 1 . \tag{19}$$

In this case ω is constant by (9), or

$$\omega = \omega_0 , \tag{20}$$

and (7), (8) give

$$\left. \begin{array}{l} u = e\alpha - \omega_0 \beta + u_0 , \\[3mm] v = -e\beta + \omega_0 \alpha + v_0 . \end{array} \right\} \tag{21}$$

5. Construction of Layouts by Analytical Method

Michell layouts are thus determined in the first place by a specification of the functions A, B as in (19) or in (16), with F(β) given a definite form, or as integrals of (13). The corresponding function ϕ is also known in each case. Cartesian equations for the layout lines can then be determined by an integration of the relations

$$\cos \phi = \frac{1}{A} \frac{\partial x}{\partial \alpha} = \frac{1}{B} \frac{\partial y}{\partial \beta} ,$$
$$\left. \sin \phi = \frac{1}{A} \frac{\partial y}{\partial \alpha} = -\frac{1}{B} \frac{\partial x}{\partial \beta} , \right\} \qquad (22)$$

which, recalling equation (1), are easily recognised as the usual formulae for the direction cosines of the tangent lines to the co-ordinate curves. Equations (22) give

$$x = \int^{(\alpha,\beta)} (A d\alpha \cos \phi - B d\beta \sin \phi) ,$$
$$\left. y = \int^{(\alpha,\beta)} (A d\alpha \sin \phi + B d\beta \cos \phi) , \right\} \qquad (23)$$

which take their simplest form when integrated along layout lines α or β constant.

Our outstanding problem is thus the determination of A, B in case (1) of paragraph 4. This requires the integration of (13), which leads to (14), or the integration of an equation of the form

$$\frac{\partial^2 H}{\partial \alpha \partial \beta} + abH = 0 . \qquad (24)$$

This can be carried out by Riemann's Method. If the value of H and one of its derivatives say $\frac{\partial H}{\partial \alpha}$ are given along a curve Γ (Fig. 4), then the other derivative $\frac{\partial H}{\partial \beta}$ is also known on Γ and the value of H at a point P (ξ, η) is also given by

$$H(P) = \frac{1}{2} \left[H(A') + H(B') \right] + \frac{1}{2} \int_{B'}^{A'} \left[\left(G \frac{\partial H}{\partial \alpha} - H \frac{\partial G}{\partial \alpha} \right) d\alpha \right.$$
$$\left. + \left(H \frac{\partial G}{\partial \beta} - G \frac{\partial H}{\partial \beta} \right) d\beta \right] ,$$
$$\qquad \ldots \ldots (25)$$

where G is a Green's Function given in our case by

$$G = J_0 \left[2\sqrt{(\alpha-\xi)(\beta-\eta)} \right] \quad \text{when } ab = +1,$$

$$G = I_0 \left[2\sqrt{(\alpha-\xi)(\beta-\eta)} \right] \quad \text{when } ab = -1,$$

$$(26)^*$$

and the points B', A' are the intersections of Γ with the α and β co-ordinate curves through P.

If the boundary values of H are given along the co-ordinate curves through the origin O where $\alpha = \beta = 0$, the value of H at point P becomes simply

$$H(\xi,\eta) = H(P) = H(O)J_0 \left(2\sqrt{ab\,\xi\eta}\right) + \int_0^\xi J_0 \left[2\sqrt{ab(\xi-\alpha)\eta}\right] \frac{\partial H}{\partial \alpha} d\alpha$$

$$+ \int_0^\eta J_0 \left[2\sqrt{ab\,\xi(\eta-\beta)}\right] \frac{\partial H}{\partial \beta} d\beta \ . \qquad (27)$$

It follows that if A, B are given respectively on a pair of intersecting co-ordinate curves, we can integrate (14) to obtain the value of A elsewhere. The value of B then follows from (13) and (23) then gives us the layout lines for the region OAPB of Fig. 4.

6. Construction of Layouts by Graphical Method

Owing to the difficulty of carrying out the integrations in equations (23) and (25), it is not always easy to construct a layout analytically. Graphical methods are however available as an alternative. It was mentioned in paragraph 3 that the geometrical properties of the layout lines of the Michell framework are identical with those of the slip-lines in plane plastic flow. The technique of graphical construction of the slip-lines, which has been very well developed for the study of the theory of plasticity (Ref. 8 VI), can thus be employed for our purpose.

---

* J_0 and I_0 are the Bessel and Modified Bessel Functions of zero order.

The most convenient method, though perhaps not the most accurate, requires the knowledge of the angle ϕ only. Integrating equation (10 gives

$$\phi = f(\alpha) + g(\beta) . \tag{28}$$

which means that the change of angle ϕ for a finite increment of α along any α-co-ordinate curve is independent of β, and the change of ϕ for a finite increment of β along any β-co-ordinate curve is independent of α. Hence, between any two co-ordinate lines of one family, the co-ordinate lines of the other family turn through a constant angle (Fig. 5). This is known as Hencky's Theorem in plane plastic flow theory and will also be called by that name in its present application.

This property enables the layout to be drawn graphically when suitable boundary conditions are given. One of the simplest cases is when two intersecting layout lines, one belonging to each family, are known.

Let the given lines OA and OB be used as the axes of a curvilinear co-ordinate system α and β respectively (Fig. 6). A point (m, n) is defined by the α and β co-ordinate lines through this point. The β-line intersects the α axis at (m, o) and the α-line intersects the β-axis at (o, n). Then by Hencky's Theorem we have

$$\phi(m, n) - \phi(o, n) = \phi(m, o) - \phi(o, o). \tag{29}$$

The fixed reference axes O(x, y) may be chosen so that they are tangential to the α, β axes at the origin O. In that case $\phi(o, o) = 0$ and (29) is simplified into

$$\phi(m, n) = \phi(m, o) + \phi(o, n) . \tag{30}$$

Since OA and OB are given, the angles $\phi(m, o)$ and $\phi(o, n)$ are known. The angle $\phi(m, n)$ at any point in the region that is defined by OA and OB can therefore be calculated from (30).

The layout lines can now be constructed approximately step by step, starting from the points (1, 0) and (0, 1). Point (1, 1) is located by drawing straight lines through these two end points, making angles with the reference directions equal to the average value of ϕ at the end points of each line (Fig. 7). The point (2, 1) can next be located from lines drawn through the point (2, 0) and (1, 1) by the same method, and so on. The layout lines in the whole region defined by OA and OB can therefore be drawn. They are approximated by broken segments of straight lines.

It may be seen that if we divide the two known curves OA and OB such that the change of angle $\Delta\phi$ between the consecutive points $(0,0)$, $(0,1)$, $(0,2) \ldots (0,n)$ and $(0,0)$, $(1,0)$, $(2,0) \ldots (m,0)$ is kept constant, the change of angle along any layout line at any intersection will also be constant and equal to $\Delta\phi$ by Hencky's Theorem (Fig. 8). This enables the whole layout to be drawn rapidly on a draughting machine without the necessity to calculate ϕ at every intersecting point. Furthermore, the configuration at every intersection is identical, an advantage which can be usefully exploited in the calculation of loads in the members of the layout.

The case when other boundary conditions are given can be resolved if an analogy with a corresponding problem in plane plastic flow can be found. The method used for the construction of the slip-lines in such a problem can then be utilised for the layout lines. The details of various other boundary value problems are given in Ref. 8.

7. Calculation of Size of Structural Members

The framework which is determined by the Michell layouts of paragraphs 5, 6 must be considered as two families of closely spaced fibres lying along the α, β co-ordinate curves, one set carrying a stress $(+f)$ and the other $(-f)$, with perhaps concentrated members along isolated lines, for example along edges. Since the structural elements are continuously distributed, their cross-sectional areas are properly described by their equivalent thickness t_1 and t_2 in the α and β directions respectively. Thus across a width $Bd\beta$ normal to the α-direction, there pass members whose total cross-sectional area is $t_1 Bd\beta$ and which transmit a total force $ft_1 Bd\beta$. Similarly, normal to the β-direction, the force on the element of width $Ad\alpha$ is $-ft_2 Ad\alpha$.

To determine t_1 and t_2, we consider the equilibrium of our two dimensional layout. Using the differential equation of equilibrium in curvilinear co-ordinates given in Ref. 10 we find, recalling (6), that

$$\frac{\partial}{\partial\alpha}(t_1 B) + t_2 A \frac{\partial\phi}{\partial\beta} = 0 , \left.\begin{array}{c}\\[2em]\end{array}\right\} \quad (31)$$

$$\frac{\partial}{\partial\beta}(t_2 A) - t_1 B \frac{\partial\phi}{\partial\alpha} = 0 .$$

For the various co-ordinate systems considered in paragraph 4, we have the following cases.

(A) Case 1.   Here equation (11) gives $\phi = a\alpha + b\beta$, and so if we write

$$T_1 = t_1 B, \qquad\qquad T_2 = t_2 A, \qquad\qquad (32)$$

equations (31) become

$$\frac{\partial T_1}{\partial \alpha} + bT_2 = 0, \quad \frac{\partial T_2}{\partial \beta} - aT_1 = 0, \qquad (33)$$

from which we deduce

$$\left.\begin{array}{l} \dfrac{\partial^2 T_1}{\partial\alpha\partial\beta} + abT_1 = 0, \\[4mm] \dfrac{\partial^2 T_2}{\partial\alpha\partial\beta} + abT_2 = 0. \end{array}\right\} \qquad (34)$$

These are in the same form as (24) and their solution can be found in the form of equation (25) or (27). Since T_1 , T_2 , A and B are now known, t_1 and t_2 can readily be found.

(B) Case 2.

If $\frac{\partial \phi}{\partial \alpha} = 0$ and the co-ordinates are as chosen in Case 2 of paragraph 4, then A = 1, B $= \alpha + F(\beta)$ and $\phi = \beta$ by equation (16). Equations (31) reduce to

$$\frac{\partial t_2}{\partial \beta} = 0, \qquad \frac{\partial}{\partial \alpha}(Bt_1) + t_2 = 0. \qquad (35)$$

Differentiating and using (32) gives

$$\frac{\partial t_2}{\partial \beta} = 0, \qquad \frac{\partial^2 T_1}{\partial\alpha\partial\beta} = 0. \qquad (36)$$

which can be integrated to give

$$\left.\begin{array}{l} T_1 = \Gamma(\alpha) + \chi(\beta), \\[4mm] t_2 = -\Gamma'(\alpha), \end{array}\right\} \qquad (37)$$

where Γ and χ are arbitrary functions which must be determined to satisfy the boundary conditions at the edge of the region.

(C) Case 3.

Finally, if α, β are taken as orthogonal co-ordinates with $A = B = 1$, $\frac{\partial \phi}{\partial \alpha} = \frac{\partial \phi}{\partial \beta} = 0$, then $t_1 = t_1(\beta)$ and $t_2 = t_2(\alpha)$. Each fibre is straight and is of constant thickness along its length. These thicknesses are again determined by the equilibrium conditions at the boundary of the region.

The equilibrium conditions at a boundary can be written using Fig. 9. Let F_n, F_t be the components of external traction per unit length in the direction of the normal and tangent respectively, and T the end load in the edge member at the boundary, if any. Let also the angle between the α -curve and the tangent to the boundary be θ, the radius of curvature of the boundary curve be ρ, and the arc length of a small element of the boundary curve be $d\sigma$. Then the components of T in the normal and tangential directions of the boundary are $-T_{/\rho}$ and $\frac{\partial T}{\partial \sigma}$. The equilibrium of forces in the α, β directions give

$$\left.\begin{array}{l} ft_1 \sin\theta = (F_n - \frac{T}{\rho}) \sin\theta + (F_t + \frac{\partial T}{\partial \sigma}) \cos\theta , \\[3mm] ft_2 \cos\theta = (F_t + \frac{\partial T}{\partial \sigma})\sin\theta - (F_n - \frac{T}{\rho}) \cos\theta . \end{array}\right\} \quad (38)$$

These equations determine the values of t_1 and t_2 at the boundary, and may be used in appropriate cases to specify the arbitrary functions of the various integrals.

The conception of a framework as two continuous sheets of fibres, although appropriate to the mathematical treatment, has little value in practical application. For one thing, the connection between the two sheets presents a formidable engineering problem. However, the graphical method of layout discussed in paragraph 6 readily suggests an approximation. We may replace the two sheets of fibres in a curvilinear element $Ad\alpha \times Bd\beta$ by two concentrated straight members along the mean α, β lines. Thus the framework consists of two sets of members arranged along the layout lines as constructed in paragraph 6, one carrying a tensile stress (f) and the other a compressive stress (-f), with pinned joints at the junctions.

Since the members are to carry direct stresses only, loads on the boundary must be considered as applied at the joints. The sizes of the members can be calculated once the forces carried by them become known. Equilibrium considerations at the joints provide such information in statically determinate cases.

8. Calculation of Volume of Michell Structures

For a framework S^* satsifying Michell's Theorem, if $\overline{F}_i (i = 1, \ldots n)$ are the external forces acting on the structure, and $\overline{v}_i$ are the virtual displacements at their points of application, the virtual work of the external forces is $\sum\limits_{i=1}^{n} \overline{F}_i \overline{v}_i$. The virtual deformation produces strains (+e) along all the members carrying a stress (+f), and (-e) along all the members carrying a stress (-f), and so the total change of strain energy in S^* is Σ (fA) (eL) $=$ ef Σ AL $=$ efV^*, where the summation is taken over all the members of area A and length L, and V^* is the total volume of the framework. By the Principal of Virtual Work, we have

$$ ef V^* = \sum_{i=1}^{n} \overline{F}_i \overline{v}_i \ , $$

or

$$ V^* = \frac{1}{fe} \sum_{i=1}^{n} \overline{F}_i \overline{v}_i \ . \tag{39} $$

The virtual displacements $\overline{v}_i$ follow from u and v of equations (15), (18) or (21) for the various co-ordinate systems. The volume of the structure can then be calculated from (39).

The knowledge of the volume of a Michell structure, when it can be found, is most valuable. It represents the ultimate structural efficiency. If for any reason the optimum structure cannot be used and another form of construction is substituted, the penalty involved is readily calculated by comparing the weight of the proposed construction with the Michell structure.

The approximate framework with concentrated members replacing the two sheets of fibres is strictly speaking one of such cases. The volume of the framework can be calculated by summing over all members once their size is known. This may be compared with the volume of (39). It may be expected that since the framework follows the exact framework in layout and differs only in the distribution of materials, the difference in weight between the two will be very small indeed.

PART II

SPECIAL APPLICATIONS

1. Development of the Solution for a Cantilever

Consider the three-force problem of Fig. 10. The points of application of the forces form an isosceles triangle CDC' with CD = C'D. The force F at D acts in a direction parallel to CC' and equal forces at C, C', directed along CD, C'D respectively, are in equilibrium with the force F. Our problem is to construct a Michell structure which equilibrates these forces.

Concentrated forces can be dealt with in two ways in Michell layouts. The point of action of such a force can be made a singular point of the layout, with an infinite number of fibres passing through (Fig. 11a); or special members, with finite cross-sectional area, can be introduced along the two layout lines which intersect at this point of action (Fig. 11b). Let us apply the first of these methods to the points C, C' of Fig. 10 and assume, as the simplest solution, that the lines which meet at C, C' are straight lines. This gives us two fans of radial lines and concentric circles centred on C and C', which may be extended until they meet at O, the vertex of an isosceles right angled triangle with hypotenuse C C' (Fig. 12).

We now have a situation familiar in the plastic flow theory. Two orthogonal layout lines OA, OB (Fig. 12) are now given and it is required to extend this layout into the region which contains the point D. This problem is solved in Ref. 8, VI.7 and the resulting layout, continued until two layout lines meet at D, is shown in Fig. 13.

Introducing concentrated members along CD, C'D we can accommodate the concentrated force at D. The member CD will be in tension and the member C'D in compression. All the members which meet at C must therefore be in tension and all those which meet at C' in compression, in accordance with the general theory of Michell structures. The curved member AD is in tension and therefore requires the compressive forces in members through C', which meet it at right angles, to maintain the equilibrium. In the same way the member BD requires the tensile forces in the members through C. The circular members in the fans centred C and C' are clearly not required and so have been omitted from Fig. 13.

The structure of Fig. 13 appears to be qualitatively satisfactory, but before it can be accepted a check must be made that suitable positive areas may be given to all its members. A similar situation arises in plasticity problems, where it is necessary to demonstrate that a consistent velocity distribution is possible. (Ref. 8, VII.1).

2. Layout Geometry

The layout lines for our cantilever structure can be taken as the co-ordinate curves of a curvilinear co-ordinate system (α, β). Referring to Fig. 14 we take the circular arc OA as the line $\beta = 0$ and define the values of α at points, such as A_1, on OA, by the angle between the tangent at A_1 and that at O, which is taken as the x-axis of a right handed Cartesian co-ordinate system O(x, y). Taking the direction O to A as positive and taking clock-wise rotations as defining positive angles, we see that the values of α on OA are all positive. The arc OB is taken as $\alpha = 0$ and the value of β for a point such as B_1 is then defined as the angle between the tangents at B_1 and O. The positive direction on $\alpha = 0$ is taken as from O to B. Taking anti-clockwise rotations as positive we see that the values of β on OB are also positive. The co-ordinates of a point P are then given by the value of α at the point A_1, where a layout line through P meets OA, and by the value of β at B_1, where the other layout line through P meets OB.

Let us denote the angle between the tangent to the α-curve through P and the x-axis by ϕ. The co-ordinate system is then the same as that in Fig. 2c and Hencky's Theorem (eq. 10) gives the relation

$$\phi = -\alpha + \beta , \tag{40}$$

which corresponds to (11) with a = -1 and b = +1.

The arc lengths ds_1, ds_2 of the α, β curves are given by $A d\alpha$, $B d\beta$ respectively. Since $d\alpha$, $d\beta$ are now numerically equal to the change of angle along the respective co-ordinate curves, A, B are the radii of curvature of α, β curves. Equations (13), (14) for A and B become in this case

$$\frac{\partial A}{\partial \beta} = B , \qquad \frac{\partial B}{\partial \alpha} = A , \tag{41}$$

and

$$\frac{\partial^2 A}{\partial \alpha \partial \beta} - A = 0 , \qquad \frac{\partial^2 B}{\partial \alpha \partial \beta} - B = 0 . \tag{42}$$

The boundary values are

$$A = \frac{\partial B}{\partial \alpha} = r \quad \text{on} \quad OA \, (\beta = 0) ,$$
$$B = \frac{\partial A}{\partial \beta} = r \quad \text{on} \quad OB \, (\alpha = 0) , \tag{43}$$

where r is the radius of the circles centred on C and C'.

The solution for A is given by equation (27) with ab = -1. We have, at a point $P(\xi, \eta)$

$$A(P) = r\, I_0\, (2\sqrt{\xi\eta}) + \int_0^\eta I_0 \left[2\sqrt{\xi\,(\eta-\beta)} \right] r\, d\beta$$

$$= r \left[I_0\, (2\sqrt{\xi\eta}) + \sqrt{\frac{\eta}{\xi}}\, I_1\, (2\sqrt{\xi\eta}) \right]$$

after transformation using the substitution $\zeta = 2\sqrt{\xi\,(\eta-\beta)}$ in the integral.

Similarly,

$$B(P) = r\, I_0\, (2\sqrt{\xi\eta}) + \int_0^\xi I_0 \left[2\sqrt{(\xi-\alpha)\eta} \right] r\, d\alpha$$

$$= r \left[I_0\, (2\sqrt{\xi\eta}) + \sqrt{\frac{\xi}{\eta}}\, I_1\, (2\sqrt{\xi\eta}) \right] .$$

Hence, at a point with current co-ordinates (α, β), the radii of curvature A, B are given by:

$$\left.\begin{aligned}
A(\alpha,\beta) &= r \left[I_0\, (2\sqrt{\alpha\beta}) + \sqrt{\frac{\beta}{\alpha}}\, I_1\, (2\sqrt{\alpha\beta}) \right] , \\
B(\alpha,\beta) &= r \left[I_0\, (2\sqrt{\alpha\beta}) + \sqrt{\frac{\alpha}{\beta}}\, I_1\, (2\sqrt{\alpha\beta}) \right] .
\end{aligned}\right\} \tag{44}$$

Equation (1) now gives the line element ds, which, together with the angle ϕ from (40), give the intrinsic equation of the co-ordinate lines in parametric form. The Cartesian co-ordinates (x, y) are given by (23). If the integration is performed along the α-lines (β = constant), starting from the arc OB, where $\alpha = 0$, equations (23) become

$$\left.\begin{aligned}
x - x_0 &= \int_0^\alpha A \cos\phi\, d\alpha , \\
y - y_0 &= \int_0^\alpha A \sin\phi\, d\alpha ,
\end{aligned}\right\} \tag{45}$$

where

$$\left.\begin{aligned}
x_{(0,\beta)} &= -r\,(1 - \cos\beta) , \\
y_{(0,\beta)} &= r\sin\beta .
\end{aligned}\right\} \tag{46}$$

It does not seem possible to get an analytical expression for x and y from (45). However values may be obtained by numerical integration, and the co-ordinate curves α, β can then be plotted. The pair of curves

which intersect at point D furnish the boundary of the structure.

3. Graphical Construction of the Layout

Following the general method discussed in paragraph 6, Part I, the layout lines can be constructed approximately on the basis of equation (40). It is particularly easy when the pair of given layout lines are circular arcs, as we have in the present case, since they can be conveniently divided into equiangular segments containing and angle $\Delta\phi$ (Fig. 15). The layout lines are the continuation of the radial lines from the centres C and C'. It can be shown that each line turns through an angle $\frac{\Delta\phi}{2}$ on leaving the circular arc, and thereafter turns through an angle $\Delta\phi$ at every intersection with the other family of lines. The two sets of co-ordinate lines then form a quadrilateral mesh. Given three corners of a quadrilateral the fourth corner can always be located. The two sets of lines can therefore be drawn step by step, starting at the three corner points 0, 1, and 1', and continuing until two lines meet at the loading point D as shown in Fig. 13. Needless to say, the smaller the angle $\Delta\phi$, the finer the mesh and the better the approximation will be.

Examples of the layouts constructed by this method are shown in Figs. 16 -18. Fig. 16 shows the layout defined by two right-angled circular arcs of equal radii and was drawn with an equiangular mesh of 5°. All the other figures have 10° meshes. Fig. 17 shows the limiting angles which two circular arcs of equal radii may subtend. These angles are seen to be just over 240°. Beyond this limit, the two systems of layout lines will overlap and will thus be unacceptable. There is therefore a definite boundary associated with a given pair of circular arcs which limits the region of the structure. The loading point D must clearly be situated inside this region. Fig. 18a - e show the layouts defined by right-angled circular arcs of different radii. The last of them (18e) shows the case when one radius becomes zero and the corresponding arc degenerates into a point.

4. Calculation of sizes of a symmetrical cantilever

Having constructed the layout, we can now calculate the sizes of the members required to carry a load F applied at D (Fig. 13). To start with, two concentrated members along the co-ordinate lines passing through D will be needed. The loads in these members at the point D is $\pm F/\sqrt{2}$, since the members intersect the line of symmetry OD at 45°. The fibres intersecting these members at right angles cannot alter the magnitude of these loads. Hence the sizes of these two members remain

constant from point D to C and C', with areas equal to $F/\sqrt{2}f$.

All members radiating from C carry a tensile stress (f) and those from C' carry a compressive stress (-f). To find the equivalent thickness t_1 and t_2 of the continuously distributed fibres we use (34) and (35), with a = -1 and b = +1 for the chosen co-ordinate system. They give

$$\frac{\partial T_1}{\partial \alpha} + T_2 = 0 \ , \qquad \frac{\partial T_2}{\partial \beta} + T_1 = 0 \ , \qquad (47)$$

and

$$\frac{\partial^2 T_1}{\partial \alpha \partial \beta} - T_1 = 0 \ , \qquad \frac{\partial^2 T_2}{\partial \alpha \partial \beta} - T_2 = 0 \ , \qquad (48)$$

where $T_1 = t_1 B$ and $T_2 = t_2 A$ as given in (32).

The boundary conditions are given by the equilibrium of the edge members. Thus on BD, we have by Fig. 19,

$$ft_2 = \frac{F}{\sqrt{2}A}$$

or $\qquad At_2 = T_2 = \frac{F}{\sqrt{2}f}$. $\qquad (49a)$

This equation can also be obtained from (38). The boundary curve coincides here with a α-curve, hence $\theta = 0$ and $\rho = A$. The components of boundary traction $F_t = F_n = 0$ and $T = F/\sqrt{2} = $ constant.

Similarly, on AD we have

$$Bt_1 = T_1 = \frac{F}{\sqrt{2}f} \ . \qquad (49b)$$

The equations (48) are of the same form as (24), with boundary conditions (49a) and (49b). Their solutions, by equations (25), give at the origin O(Fig. 20)

$$T_1(O) = \frac{F}{\sqrt{2}f} \ I_0 (2\sqrt{\xi \eta}) - \int_B^D (-\frac{F}{\sqrt{2}f}) I_0 (2\sqrt{\alpha \eta}) d\alpha$$

$$= \frac{F}{\sqrt{2}f} \left[I_0 (2\sqrt{\xi \eta}) + \sqrt{\frac{\xi}{\eta}} \ I_1 (2\sqrt{\xi \eta}) \right] \ . \qquad (50a)$$

and
$$T_2(O) = \frac{F}{\sqrt{2}f}\left[\; I_0\;(2\sqrt{\xi\eta}) + \sqrt{\frac{\eta}{\xi}}\; I_1\;(2\sqrt{\xi\eta})\;\right] \; . \tag{50b}$$

The values of T_1 and T_2 at a point $P(\alpha,\beta)$ can be obtained by making P the origin instead of O. The co-ordinates of D then become $(\xi-\alpha,\ \eta-\beta)$. Hence from (50),

$$T_1(\alpha,\beta) = \frac{F}{\sqrt{2}f}\left\{\; I_0\left[\;2\sqrt{(\xi-\alpha)(\eta-\beta)}\;\right] + \sqrt{\frac{\xi-\alpha}{\eta-\beta}}\; I_1\left[2\sqrt{(\xi-\alpha)(\eta-\beta)}\right]\right\},$$

$$T_2(\alpha,\beta) = \frac{F}{\sqrt{2}f}\left\{\; I_0\left[\;2\sqrt{(\xi-\alpha)(\eta-\beta)}\;\right] + \sqrt{\frac{\eta-\beta}{\xi-\alpha}}\; I_1\left[2\sqrt{(\xi-\alpha)(\eta-\beta)}\right]\right\}. \tag{51}$$

Therefore, at any point in the region of OABD, we can calculate T_1, T_2 by (51) and A, B by (44). The equivalent thicknesses are then given by (33). Since T_1, T_2, A and B are always positive, the same is true for t_1 and t_2 and the solution is therefore acceptable.

The values of $\dfrac{\sqrt{2}\,fr\,t_2}{F}$ in a region defined by two right-angled circular arcs are plotted in Fig. 21. The same figure can be used to find values of $\dfrac{\sqrt{2}\,fr\,t_1}{F}$ by interchanging α and β. The position of the points A and B in the figure will then be interchanged.

The layout lines within the circular arc OB are radial lines from centre C and concentric arcs, forming a fan structure. Since there is no load on the edge of the fan, no material is required along the arcs. Each tensile element from the arc OB will continue radially towards the singular point C with an unchanged area of section. The same applies to the compression material in the fan C'OA.

The cantilever structure therefore consists of two concentrated edge members CD and C'D of constant areas, a continuum of tensile material spreading from the singular point C to the edge AD, and a similar continuum of compression material in the region C'BD. The sizes of these structural elements has been determined.

For the approximate framework with concentrated members replacing the continuous sheets, the sizes of the members are known once the loads they carry are calculated. These can be found by consideration of the equilibrium at every joint, starting from the loading point D. The structure is statically determinate, since it is built up by

adding two members to every joint, starting from the tip D. It is also to be noticed that if the layout lines form an equiangular network, the configuration at every joint of one or other of two similar types is the same. The forces in the members can therefore be calculated by using the same formulae throughout the whole region. Furthermore, for a symmetrical layout with a load applied normal to the axis of symmetry, only one half of the structure needs to be considered.

We consider only the top half of the structure, where the edge member BD is in tension. At point D, where the two members intersect the axis of symmetry at angles $\left(\dfrac{\pi}{4} - \dfrac{\Delta\phi}{2}\right)$ (Fig. 22a), the forces in the members are $\pm\dfrac{F}{2 \sin\left(\dfrac{\pi}{4} - \dfrac{\Delta\phi}{2}\right)}$ (compared with $\pm\dfrac{F}{\sqrt{2}}$ in the exact structure). The forces in the rest of the members can now be calculated from joint to joint, knowing always the tension T in the member nearest to D, and the compression C in the member nearest to the edge BD. There are two types of joints in the region according to their position.

(a) For joints outside the arc OB, the geometry is shown in Fig. 22b. The unknown force in the tensile member is

$$T' = T \sec \Delta\phi + C \tan \Delta\phi \quad , \tag{52a}$$

and in the compression member

$$C' = C \sec \Delta\phi + T \tan \Delta\phi \quad . \tag{52b}$$

(b) For joints on OB, the geometry is slightly different (Fig. 22c). The unknwon forces are given by

$$T' = T \sec \frac{\Delta\phi}{2} + 2C \sin \Delta\phi \quad , $$
$$C' = C + T \tan \frac{\Delta\phi}{2} \quad . \tag{53}$$

The joints on the edge BD have the same geometry, the only difference being that C = 0.

An example of the calculation is given in Fig. 23, where the forces in the members due to a unit load F at D are shown. The structure is an equiangular layout, with $\Delta\phi = 10^{\circ}$, defined by two right-angled circular arcs. The forces on the edge member from D to C now increase gradually instead of remaining constant as in the exact structure.

5. Calculation of Virtual Displacements and Volume

Equation (39) gives the volume V^* of the Michell structure which is proportional to the virtual work of the external forces. In our cantilever there is only one force applied and we have to find the virtual displacement in the direction of this force.

Equation (15) gives the components of the virtual displacement u, v in the direction of α, β co-ordinate curves. For the co-ordinate system chosen, we have a = -1 and b = +1. Hence the equations become

$$\frac{\partial u}{\partial \alpha} + v = Ae \, , \qquad \frac{\partial u}{\partial \beta} - v = -B\omega \, , \left.\begin{matrix}\\ \\ \\ \\ \end{matrix}\right\} \tag{54}$$

$$\frac{\partial v}{\partial \alpha} - u = A\omega \, , \qquad \frac{\partial v}{\partial \beta} + u = -Be \, ,$$

where

$$\omega = -2e(\alpha+\beta) + \omega_o \tag{55}$$

which follows from (12).

Adding the equations (54) in pairs we arrive at the following results :

$$\frac{\partial u}{\partial \alpha} + \frac{\partial u}{\partial \beta} = Ae - \beta\omega \, , \left.\begin{matrix}\\ \\ \\ \end{matrix}\right\} \tag{56}$$

$$\frac{\partial v}{\partial \alpha} + \frac{\partial v}{\partial \beta} = -Be + A\omega,$$

where A, B are functions of α, β given by (44).

We now change the variables and let

$$\sigma = \alpha + \beta \, , \qquad \tau = \alpha - \beta \, . \tag{57}$$

The lines σ = constant and τ = constant, when drawn in the α, β plane, intersect the α, β co-ordinate lines at 45°. These lines can be regarded as a new set of co-ordinate lines (Fig. 24). The origin of the σ, τ co-ordinate system remains at O. The positive σ-axis lies in the first quadrant while the positive τ-axis lies in the fourth quadrant of the α, β plane, thus forming a left-handed system.

From (57), we have the inverse transformation

$$\alpha = \frac{1}{2}(\sigma + \tau) \, , \qquad \beta = \frac{1}{2}(\sigma - \tau) \, , \tag{58}$$

and also
$$\frac{\partial u}{\partial \alpha} = \frac{\partial u}{\partial \sigma} + \frac{\partial u}{\partial \tau} \quad ,$$

$$\frac{\partial u}{\partial \beta} = \frac{\partial u}{\partial \sigma} - \frac{\partial u}{\partial \tau} \quad ,$$
(59)

and similarly for $\dfrac{\partial v}{\partial \alpha}, \dfrac{\partial v}{\partial \beta}$.

Equations (56) then become

$$2\frac{\partial u}{\partial \sigma} = Ae - B\omega, \qquad 2\frac{\partial v}{\partial \sigma} = -Be + A\omega \, ,$$
(60)

where A and B are now to be expressed as functions of σ and τ by (44) and (58). These two equations can be integrated along the σ-lines (τ = constant) starting from a boundary where u (or v) is given.

For our cantilever structure, the centres of the circular fans C and C' can be regarded as fixed. The virtual deformation imposes a strain (+e) on all tensile members and (-e) on all compression members. Hence, on the arc OB at a radius r from the centre, the virtual displacement u in the direction of the α-lines is (er). Similarly v on OA is (-er), the negative sign indicates that the direction of the displacement is opposite to the positive direction of the β-lines. These are then the boundary conditions for (60).

The value of ω_o in (55) is the rotation at the origin when $\alpha = \beta = 0$. At the origin of our co-ordinate system $A = B = r$, $u = -v = er$, and $\dfrac{\partial u}{\partial \beta} = \dfrac{\partial v}{\partial \alpha} = 0$. Hence by (54), we have

$$\omega_o = -e \, .$$
(61)

Substituting (44), (55), (58) and (61) into (60) gives

$$
\begin{aligned}
2\,\frac{\partial u}{\partial \sigma} &= er\left[I_o\left(\sqrt{\sigma^2-\tau^2}\right) + \sqrt{\frac{\sigma-\tau}{\sigma+\tau}}\, I_1\left(\sqrt{\sigma^2-\tau^2}\right) \right] \\
&\quad + (2e\sigma + e)r\left[I_o\left(\sqrt{\sigma^2-\tau^2}\right) + \sqrt{\frac{\sigma+\tau}{\sigma-\tau}}\, I_1\left(\sqrt{\sigma^2-\tau^2}\right) \right] , \\
2\,\frac{\partial v}{\partial \sigma} &= -er\left[I_o\left(\sqrt{\sigma^2-\tau^2}\right) + \sqrt{\frac{\sigma+\tau}{\sigma-\tau}}\, I_1\left(\sqrt{\sigma^2-\tau^2}\right) \right] \\
&\quad - (2e\sigma + e)r\left[I_o\left(\sqrt{\sigma^2-\tau^2}\right) + \sqrt{\frac{\sigma-\tau}{\sigma+\tau}}\, I_1\left(\sqrt{\sigma^2-\tau^2}\right) \right] .
\end{aligned}
$$
(62)

Integration of (62) gives u, v at any point $P(\alpha, \beta)$ in the structure. The details of the integration are presented in Appendix A and the result gives

$$u(\alpha, \beta) = er\left[(1 + 2\alpha) I_0 (2\sqrt{\alpha\beta}) + 2\sqrt{\alpha\beta} I_1 (2\sqrt{\alpha\beta})\right],$$
$$v(\alpha, \beta) = -er\left[(1 + 2\beta) I_0 (2\sqrt{\alpha\beta}) + 2\sqrt{\alpha\beta} I_1 (2\sqrt{\alpha\beta})\right]. \qquad (63)$$

Let the co-ordinates of the loading point D be $(\alpha = \mu, \beta = \mu)$, then

$$u(D) = -v(D) = er\left[(1 + 2\mu)I_0 (2\mu) + 2\mu I_1(2\mu)\right]. \qquad (64)$$

The virtual displacement in the direction of the applied force F, which makes angles of $\dfrac{\pi}{4}$ and $\dfrac{3\pi}{4}$ with the α, β co-ordinate curves at D, is

$$\bar{v} = u(D) \cos\frac{\pi}{4} - v(D) \sin\frac{\pi}{4} = \sqrt{2}\ u(D). \qquad (65)$$

The volume of the structure then follows from (39), giving

$$V^* = \frac{F\bar{v}}{fe} = \frac{\sqrt{2}Fr}{f}\left[(1 + 2\mu) I_0 (2\mu) + 2\mu I_1 (2\mu)\right]. \qquad (66)$$

For the framework with concentrated members replacing the continuous sheets, the total volume V is the sum of the volumes of all the members, which are known once the loads are calculated and their length measured. It has been calculated for a number of symmetrical cantilever layouts, and the following table gives the results compared with those obtained by (66) for the 'exact' structure.

μ (degrees)	$\dfrac{V^{*}f}{Fr}$ (eq. 66)	$\dfrac{Vf}{Fr}$ (for framework with concentrated members)
0	1.414	1.414
10	2.053	2.056
20	3.070	3.065
30	4.632	4.634
40	6.994	7.02
50	10.53	10.57
60	15.80	15.89
70	23.61	23.76
80	35.12	35.39
90	52.04	52.56
100	76.87	77.80
110	113.20	114.78

In spite of the fact that a coarse network ($\Delta\phi = 10^{\circ}$) has been used, the volume obtained by the approximate calculation is within 1.5% of that for the exact theory, even when the angle of the fans is as large as 110°. The closeness of the agreement is remarkable and the approximate method of analysis can therefore be considered as highly satisfactory.

6. Comparison of the Weight of Michell Cantilever with that of other types of Cantilever Structures.

The volume of the Michell framework is plotted in the form of the non-dimensional quantity $\dfrac{Vfd}{F\ell^2}$ against the ratio of $\dfrac{\ell}{d}$ in Fig. 25. The distance d is the depth between the singular points CC' and ℓ is the span of the cantilever from the root CC' to the loading point D. The length ℓ has been measured directly from the layout drawings.

In the same figure, the volumes of three other types of conventional cantilever structures having length ℓ and depth d at the base are also plotted. All the allowable tensile and compressive stresses are assumed

- 24 -

to be ±f, and the load F is applied at a point D on the perpendicular bisector of CC'. The volumes are calculated as follows:

(A) For the simple triangular structure consisting of a tie CD and a strut C'D (Fig. 26a), the volume is

$$V = 2 \frac{F}{f} \frac{(\ell^2 + d^2/4)}{d} \; ,$$

hence

$$\frac{Vfd}{F\ell^2} = 2 \left(1 + \frac{d^2}{4\ell^2} \right) \tag{67}$$

(B) The simple webbed-beam (Fig. 26b) with parallel spars carrying end loads and a web carrying uniform pure shear is assumed to be fixed at C and C' so as to make it strictly comparable with the Michell framework. A shear post is therefore necessary at each end. The allowable stress in the web is assumed to be f/2. The volumes of the items are

$$\text{spars} \qquad V_f = 2 \times \frac{F\ell^2}{2fd} \; ,$$

$$\text{web} \qquad V_w = \frac{2F\ell}{f} \; ,$$

$$\text{and shear posts} \qquad V_s = 2 \times \frac{Fd}{4f} \; .$$

The total volume $V = V_f + V_w + V_s$ and hence

$$\frac{Vfd}{F\ell^2} = 1 + 2\frac{d}{\ell} + \frac{d^2}{2\ell^2} \; . \tag{68}$$

(C) For the Warren girder (Fig. 26c), the volume can be calculated from

$$\frac{Vfd}{F\ell^2} = \frac{3.464}{n^2} \left[1.154 \left(\frac{n^2}{4} + n \right) + 0.433 \right] , \tag{69}$$

where n = number of joints outside the supports C and C'. The value 0.433 in the bracket gives the contribution of the link from the last joint of the structure to the loading point D at the centre.

Strictly speaking, the Warren girder can only be built when ℓ and d satisfy the relation $\ell = 0.577nd$, where n is an integer. A continuous

curve is nevertheless drawn through these points to represent the volume of this type of structure.

The curves in Fig. 25 show the superiority of the Michell framework over the conventional type of structure, especially at large values of ℓ/d.

7. Application to a Beam under Uniform Bending Moment

Another application of the layout has been suggested by H. L. Cox. The layout lines defined by two equal fans OCB and OC'A are continued until the tangents of the α-line CBE and the β-line C'AE' are parallel to the axis of symmetry at the points E and E' (Fig. 27). The line joining E and E' is then tangential to the α-line CE' and the β-line C'E and is perpendicular to the axis of symmetry. The layout is now joined to another which is its own image about the line EE'. Let the singular points of this image layout be F and F', the line CEF is then a continuous curve. The two lines C'E and F'E are both normal to CEF at E and form a cusp. The length of the layout from CC' and FF' is governed by the angles of the fans.

If a moment is now applied at each end in the form of a set of equal and opposite forces at the singular points C, C', and F, F', it can be carried by a structure placed along this double system of layout lines (Fig. 28). It is easy to see that the sets of lines from C and F are in tension and those from C' and F' are in compression. At the centre section EE', the moment produces a pair of equal and opposite forces at E and E' parallel to the line of symmetry OO'. Since EE' is a line of symmetry, our attention may be confined to one half of the structure from CC' to EE'. If the distance between E and E' is d', then the forces at these points due to a moment M are $\pm M/d'$. The calculation of sizes of members can now be started from these two corners in exactly the same manner as for the cantilever. The same kind of approximate framework with concentrated members can also be constructed.

The weight of the beam can be estimated by using (39) for the volume and (63) for the virtual displacements u and v. The forces are applied in the same direction as u at E and (-v) at E'. These two displacements are equal and opposite by symmetry. The volume of half of the structure is therefore

$$\frac{V^*}{2} = \frac{2Fu(E)}{fe} = \frac{2Mu(E)}{d'fe} \ ,$$

or in non dimensional form

$$\frac{V^*f}{2M} = \frac{2u(E)}{d'e} \quad . \tag{70}$$

The quantity $\frac{V^*f}{2M}$ corresponds directly with $\frac{W}{2Pd}$ in Fig. 4 of Ref. 3, where beams under pure bending were considered. This figure is reproduced in Fig. 29 with an additional curve which is calculated according to (70). The depth d' and length ℓ used in the calculated are measured from the layout drawings and are therefore approximate. Comparison shows that for large values of ℓ/d, our layout has an advantage over even the more efficient beams proposed in Ref. 3.

In the calculation of the volume of half of the beam, we have assumed that the singular points C and C' are fixed, and the points E and E' are allowed to move. But in order to match the displacements of the two halves of the beam, E and E' must be brought back to rest. To do so we notice that when C and C' are fixed, the displacements of E and E' are anti-symmetrical. The vertical displacements of the two points are the same and in the same direction, while the horizontal displacements are equal and opposite. They can therefore be brought back to their original position by a rigid body rotation about a point on the axis of symmetry OO', plus a rigid body translation in the vertical direction. These rigid body movements have no effect on the calculation of the volume.

The Michell Theorem demands that the strain must not exceed (e) along any linear element in the region of the structure. This requirement is not fulfilled in the central region EGE'G'. In fact it can be shown (Appendix B) that in the cusp formed by the lines C'GE and F'G'E, the strain along a linear element near the point E parallel to the horizontal line OO' is infinite. This region must therefore be excluded from the permissible region for the structural layout, and the two halves of the beam join together at the singular points E and E' only. This exclusion of the central region leaves open the question as to whether a lighter beam could not be constructed, if members were allowed to lie in it.

Acknowledgement

References

1.   Michell, A. G. M.   The limit of economy of material in frame structures.
Phil. Mag., Series VI, vol. 8, 1904.

2.   Cox, H. L.   The theory of design.
A. R. C. 19,791, 1958.

3.   Cox, H. L.   Structures of minimum weight: The basic theory of design applied to the beam under pure bending.
A. R. C. 19,785, 1958.

4.   Hemp, W. S.   Theory of structural design.
C. of A. Report 115, 1958.

5.   Drucker, D. C., Shield, R. T.   Design of minimum weight.
9th International Congress of Applied Mechanics. Book 5. University of Brussels, 1957, pp 212-222.

6.   Prager, W.   On a problem of optimum design.
Brown University, Division of Applied Maths., Technical Report 38, 1958.

7.   Geiringer, H.   Fondments mathematique de la theorie des corps plastiques isotropes.
Mem. Science Mathematique. Fasicule 86. Paris, 1937.

8.   Hill, R.   Mathematical theory of plasticity.
Oxford, Clarendon Press, 1950.

9.   Prager, W.   An introduction to plasticity.
Addison-Wesley, Reading, Mass., 1959.

10.   Love, A. E. H.   A treatise on the mathematical theory of elasticity.
Cambridge, University Press, 1927.

APPENDIX A

Calculation of Virtual Displacements for the

Michell Cantilever

To find the virtual displacement u at a point $P(\alpha, \beta)$, within the region ODB of Fig. 24, we integrate the first equation of (62) along a σ-line from a point Q on OB, where the boundary condition $u = er$ is given. Let the α, β co-ordinates of Q be $(0, \eta)$, the σ, τ co-ordinates of Q are then $(\eta, -\eta)$ by (57). Since P lies on the same σ-line as Q, the value of τ at P must also be $(-\eta)$. We notice also that on this line $\sigma > \eta$. The first equation of (62) therefore becomes

$$2\left(\frac{\partial u}{\partial \sigma}\right)_{\tau = -\eta} = er\left[I_0\left(\sqrt{\sigma^2 - \eta^2}\right) + \sqrt{\frac{\sigma + \eta}{\sigma - \eta}}\ I_1\left(\sqrt{\sigma^2 - \eta^2}\right)\right]$$

$$+ (2e\sigma + e)r\left[I_0\left(\sqrt{\sigma^2 - \eta^2}\right) + \sqrt{\frac{\sigma - \eta}{\sigma + \eta}}\ I_1\left(\sqrt{\sigma^2 - \eta^2}\right)\right]$$

$$= 2er\left[I_0\left(\sqrt{\sigma^2 - \eta^2}\right) + \frac{\sigma}{\sqrt{\sigma^2 - \eta^2}}\ I_1\left(\sqrt{\sigma^2 - \eta^2}\right)\right]$$

$$+ 2er\ \sigma\left[I_0\left(\sqrt{\sigma^2 - \eta^2}\right) + \frac{\sigma - \eta}{\sqrt{\sigma^2 - \eta^2}}\ I_1\left(\sqrt{\sigma^2 - \eta^2}\right)\right].$$

$$\ldots\ldots \quad (A1)$$

Integrating along the σ-line from Q to P, we have

$$u(P) - u(Q) = er\int_\eta^\sigma \left\{ I_0\left(\sqrt{\sigma^2 - \eta^2}\right) + \frac{\sigma}{\sqrt{\sigma^2 - \eta^2}}\ I_1\left(\sqrt{\sigma^2 - \eta^2}\right) \right.$$

$$\left. + \sigma\left[I_0\left(\sqrt{\sigma^2 - \eta^2}\right) + \frac{\sigma - \eta}{\sqrt{\sigma^2 - \eta^2}}\ I_1\left(\sqrt{\sigma^2 - \eta^2}\right)\right] \right\}d\sigma.$$

$$\ldots\ldots \quad (A2)$$

Now let $\quad \zeta^2 = \sigma^2 - \eta^2$, $\qquad\qquad\qquad\qquad\qquad$ (A3)

Then $\quad \zeta d\zeta = \sigma d\sigma \qquad$ and

when $\quad \sigma = \eta$, $\qquad \zeta = 0$;

$\qquad\quad \sigma = \sigma$, $\qquad \zeta = \bar{\zeta} = \sqrt{\sigma^2 - \eta^2}$.

The terms in (A2) give

$$\int_{\eta}^{\sigma} \frac{\sigma}{\sqrt{\sigma^2 - \eta^2}} \, I_1(\sqrt{\sigma^2 - \eta^2}) d\sigma = \int_{0}^{\bar{\zeta}} \frac{\zeta I_1(\zeta) d\zeta}{\zeta}$$

$$= \left[I_0(\zeta) \right]_{0}^{\bar{\zeta}} = I_0(\sqrt{\sigma^2 - \eta^2}) - 1.$$

$$\int_{\eta}^{\sigma} \sigma I_0(\sqrt{\sigma^2 - \eta^2}) d\sigma = \int_{0}^{\bar{\zeta}} \zeta I_0(\zeta) d\zeta = \left[\zeta I_1(\zeta) \right]_{0}^{\bar{\zeta}}$$

$$= \sqrt{\sigma^2 - \eta^2} \, I_1(\sqrt{\sigma^2 - \eta^2}) \, .$$

$$\int_{\eta}^{\sigma} \frac{\sigma^2}{\sqrt{\sigma^2 - \eta^2}} \, I_1(\sqrt{\sigma^2 - \eta^2}) d\sigma = \int_{\eta}^{\sigma} \sigma \, d \left[I_0(\sqrt{\sigma^2 - \eta^2}) \right]$$

$$= \left[\sigma I_0(\sqrt{\sigma^2 - \eta^2}) \right]_{\eta}^{\sigma} - \int_{\eta}^{\sigma} I_0(\sqrt{\sigma^2 - \eta^2}) d\sigma$$

$$= \sigma I_0(\sqrt{\sigma^2 - \eta^2}) - \eta - \int_{\eta}^{\sigma} I_0(\sqrt{\sigma^2 - \eta^2}) d\sigma \, .$$

Substituting these into (A2) we have

$$u(P) - u(Q) = er \left[-1 + (1 + \sigma - \eta) I_0(\sqrt{\sigma^2 - \eta^2}) + \sqrt{\sigma^2 - \eta^2} \, I_1(\sqrt{\sigma^2 - \eta^2}) \right] \, .$$

But $u(Q) = er$, hence

$$u(P) = er \left[(1 + \sigma - \eta) I_0(\sqrt{\sigma^2 - \eta^2}) + \sqrt{\sigma^2 - \eta^2} \, I_1(\sqrt{\sigma^2 - \eta^2}) \right] \, .$$
$$\dots \dots \text{(A4)}$$

Now transforming back into α, β co-ordinates, we have $\sigma = \alpha + \beta$, and along this σ-line, $\tau = -\eta = \alpha - \beta$. Hence $\sqrt{\sigma^2 - \eta^2} = 2\sqrt{\alpha\beta}$. Substituting these into (A4) gives

$$u(\alpha, \beta) = er \left[(1 + 2\alpha) I_0(2\sqrt{\alpha\beta}) + 2\sqrt{\alpha\beta} \, I_1(2\sqrt{\alpha\beta}) \right] . \quad \text{(A5)}$$

Similarly, the virtual displacement v at a point P' in the region OAD (Fig. 24) can be found by a line integration of the second equation of (62) from a point Q' on OA on the same σ-line. The α, β co-ordinates of Q' are (ξ, o) and so its σ, τ co-ordinates are (ξ, ξ). The σ, τ co-ordinates

of P' are then (σ, ξ) where $\sigma > \xi$. The formulae of A1-4 are then applicable with u changed into v, η into ξ, and e into (-e). The integration is now performed on a σ-line with $\tau = \xi$. The corresponding formula of (A5) is then

$$v(\alpha, \beta) = -er\left[(1 + 2\beta) I_0 (2\sqrt{\alpha\beta}) + 2\sqrt{\alpha\beta} I_1(2\sqrt{\alpha\beta}) \right]. \quad (A6)$$

Equations (A5) and (A6) give the values of u in the region BOD and v in AOD, resulting from a known u on OB and v on OA. The values of u in AOD and v in BOD can be obtained from (54) by integrating along the α or β lines. The details of these integrations are omitted but when they are carried out, the resulting expressions for u and v are found to be identical with those given in (A5) and (A6). These two formulae can therefore be applied to the whole region of the structure as given in (63).

It is interesting to note that we can obtain u and v from the pair of equations (see eq. 54).

$$\frac{\partial u}{\partial \alpha} + v = Ae \quad ,$$

$$\frac{\partial v}{\partial \beta} + u = -Be \quad ,$$

where A and B are known functions of α, β. Differentiating and substituting from (41) we get

$$\left. \begin{array}{l} \dfrac{\partial^2 u}{\partial \alpha \partial \beta} - u = 2 Be \quad , \\[2ex] \dfrac{\partial^2 v}{\partial \alpha \partial \beta} - v = -2 Ae \quad . \end{array} \right\} \qquad (A7)$$

These differential equations are second order and are of the same form as (24). They can be integrated by Riemann's method and the resulting expressions are identical with those given in (A5) and (A6).

APPENDIX B

Strain in the Cusp GEG' of Fig. 27

Let the axis of symmetry of the beam OO' be the horizontal axis of a Cartesian co-ordinate system O(H, V) and denote virtual displacements referred to these axes by u_h and u_v (Fig. 27). Let the angle from the H-axis to the tangent of the α-line be θ (counter-clockwise being positive). Then

$$\theta = \phi - \frac{\pi}{4} = -\alpha + \beta - \frac{\pi}{4} . \tag{B1}$$

We will now try to find the strain along a linear element near the point E parallel to the H-axis in the cusp formed by the lines GE and G'E. To do so, we have to find the rate of change of the horizontal displacement u_h, and the rate of change of the horizontal length of the line element, along the β-line GE near the singular point E.

When the structure is fixed at C and C', the virtual displacements u_h and u_v are

$$\left. \begin{array}{l} (u_h)_0 = u \cos \theta - v \sin \theta , \\[2mm] (u_v)_0 = v \cos \theta + u \sin \theta , \end{array} \right\} \tag{B2}$$

where u and v are given by (63).

In order to match the displacements of the two halves of the beam, the points E and E' must be brought back to rest by a rigid body translation in the vertical direction and a rigid body rotation about a point on OH. The centre of rotation can conveniently be chosen at the origin O. The actual displacements u_h and u_v can be written as

$$\left. \begin{array}{l} u_h = (u_h)_0 - C_1 V , \\[2mm] u_v = (u_v)_0 + C_1 H + C_2 . \end{array} \right\} \tag{B3}$$

where C_1 is proportional to the rotation and C_2 the vertical translation, making u_h and u_v zero at point E. We find

$$C_1 = \left[\frac{(u_h)_0}{V} \right]_E , $$

$$C_2 = - \left[(u_v)_0 + C_1 H \right]_E . \tag{B4}$$

Using the first equation of (B3), we have, along the β-line C'GE,

$$\frac{\partial u_h}{\partial \beta} = \frac{\partial (u_h)_o}{\partial \beta} - C_1 \frac{\partial V}{\partial \beta} . \tag{B5}$$

The H, V co-ordinates are related to the x, y co-ordinates by

$$H = \frac{1}{\sqrt{2}} (x + y) ,$$

$$V = \frac{1}{\sqrt{2}} (y - x) . \tag{B6}$$

Hence

$$\frac{\partial V}{\partial \beta} = \frac{1}{\sqrt{2}} \left(\frac{\partial y}{\partial \beta} - \frac{\partial x}{\partial \beta} \right) . \tag{B7}$$

Now from (22),

$$\frac{\partial y}{\partial \beta} = B \cos \phi , \quad \frac{\partial x}{\partial \beta} = - B \sin \phi , \tag{B8}$$

hence

$$\frac{\partial V}{\partial \beta} = \frac{B}{\sqrt{2}} (\cos \phi + \sin \phi), \tag{B9}$$

where B is given in (44).

Differentiating the first of eq. (B2) we obtain

$$\frac{\partial (u_h)_o}{\partial \beta} = \frac{\partial}{\partial \beta} (u \cos \theta - v \sin \theta)$$

$$= \left(\frac{\partial u}{\partial \beta} - v \right) \cos \theta - \left(\frac{\partial v}{\partial \beta} + u \right) \sin \theta . \tag{B10}$$

But

$$\frac{\partial v}{\partial \beta} + u = - Be, \text{ and}$$

$$\frac{\partial u}{\partial \beta} - v = - B\omega = Be(2\alpha + 2\beta + 1)$$

by equations (54), (55) and (61), hence

$$\frac{\partial (u_h)_o}{\partial \beta} = eB \left[\sin \theta + (2\alpha + 2\beta + 1) \cos \theta \right] . \tag{B11}$$

At a point E, the tangent to the α-line is parallel to the H-axis. Hence $\theta = 0$ and $\phi = \dfrac{\pi}{4}$, and equations (B9), (B11) give

$$\left(\frac{\partial V}{\partial \beta}\right)_E = (B)_E \,,$$

$$\left[\frac{\partial (u_h)_o}{\partial \beta}\right]_E = e(B)_E \, (2\alpha + 2\beta + 1)_E \,.$$

Then by equations (B4) and (B5),

$$\left[\left(\frac{\partial u_h}{\partial \beta}\right)\right]_E = e(B)_E \left[(2\alpha + 2\beta + 1) - \frac{(u_h)_o}{eV}\right]_E . \tag{B12}$$

The quantity in the square bracket is generally not zero. For example, when the co-ordinates of the point E are $\alpha = 60^o$ and $\beta = 105^o$, $2\alpha + 2\beta + 1 = 6.76$. It is also found by (B1), (B2) and (63) that

$$(u_h)_o = u = 21.48 \text{ er.}$$

The vertical distance V is measured from the layout drawing and found to be 3.8 r. Hence

$$(2\alpha + 2\beta + 1) - \frac{(u_h)_o}{eV} = 6.76 - \frac{21.48}{3.8} = 1.10 \,,$$

which shows that $\dfrac{\partial u_h}{\partial \beta}$ at E as given by (B.12) is generally finite.

Next let the horizontal distance from a point on the β-line C'GE to the vertical ine EE' be ϵ (Fig. 30). Near the point E, the change $d\epsilon$ due to a small change $d\beta$ is represented by the distance PQ. By simple geometry, we can see that approximately $d\epsilon = PE.\,d\beta$, or $\dfrac{d\epsilon}{d\beta}$ is of the order of PE. But PE $= Bd\beta$, where B is the radius of curvature, and is of small order when $d\beta$ is small. Hence near the point E $\dfrac{d\epsilon}{d\beta}$ is of the same order as $d\beta$.

The fact that $\left(\dfrac{d\epsilon}{d\beta}\right)_E \to 0$ while $\left(\dfrac{du_h}{d\beta}\right)_E$ is finite means that the strain along a horizontal line element becomes infinite in the cusp near the point E. This violates the Michell Theorem and the region must therefore be excluded from the region available for the structural layouts.

FIG. I.

(a) $\phi = \alpha + \beta$

(b) $\phi = \alpha - \beta$

(c) $\phi = -\alpha + \beta$

(d) $\phi = -\alpha - \beta$

FIG. 2.

INVOLUTES

α, x

(α, β)

$(\beta = 0)$

α

$(\alpha = 0)$

β

β

O

EVOLUTE

FIG. 3.

β

B B' $P(\delta, \gamma)$

Γ

A'

O A x

FIG. 4.

α — LINES

$\Delta\phi$

$\Delta\phi$

β LINES

$\Delta\phi$

$\Delta\phi$

FIG. 5.

β

B (m, n)

$(0, n)$

$(0, 2)$

$(0, 1)$ $(1, 1)$ $(2, 1)$

O

$(0, 0)$ $(1, 0)$ $(2, 0)$ A

$(m, 0)$ α

FIG. 6.

$$\bar{\phi} = \tfrac{1}{2} \left(\phi(0,1) + \phi(1,1) \right)$$

$$\bar{\phi} = \tfrac{1}{2} \left(\phi(1,0) + \phi(1,1) \right)$$

FIG. 7.

FIG. 8.

$$T + \frac{\delta T}{\delta \sigma} d\sigma$$

$F_t \, d\sigma$

$ft_2 \, (d\sigma \cos \theta)$

$ft_1 \, (d\sigma \sin \theta)$

FIG. 9.

FIG. 10.

(a)   (b)
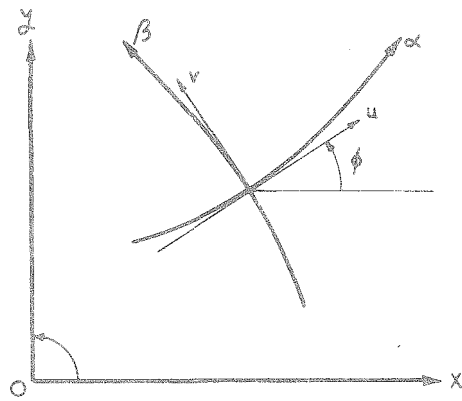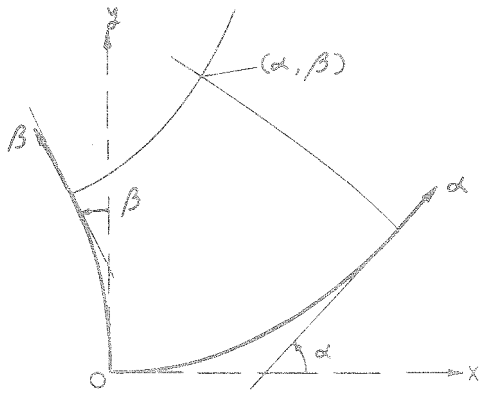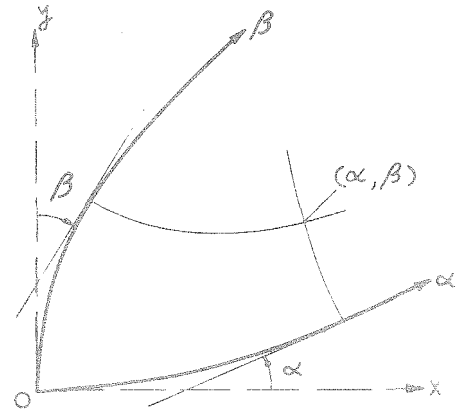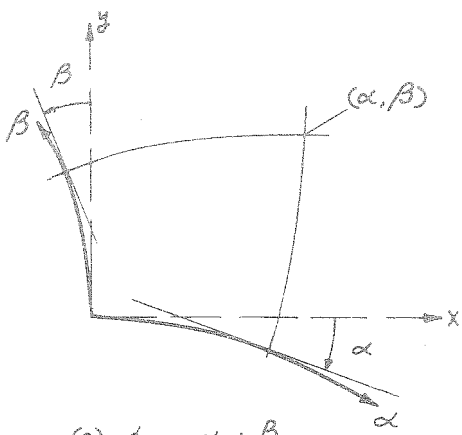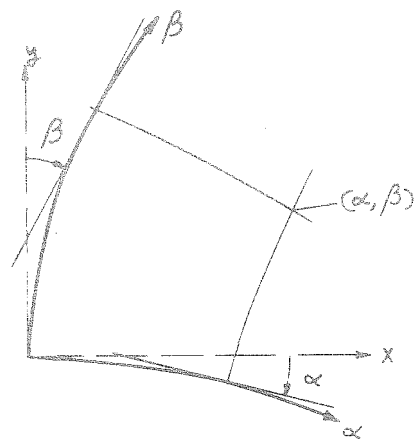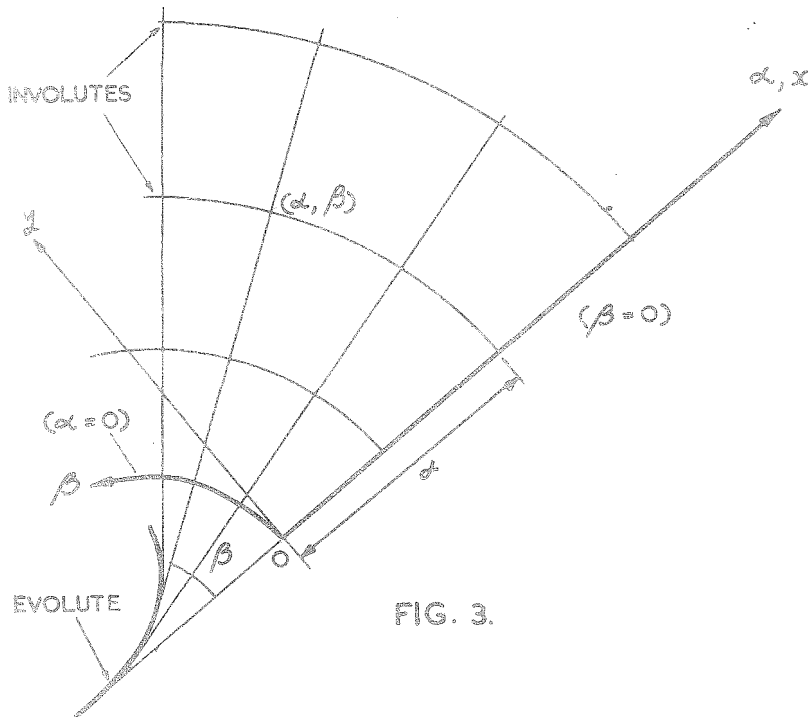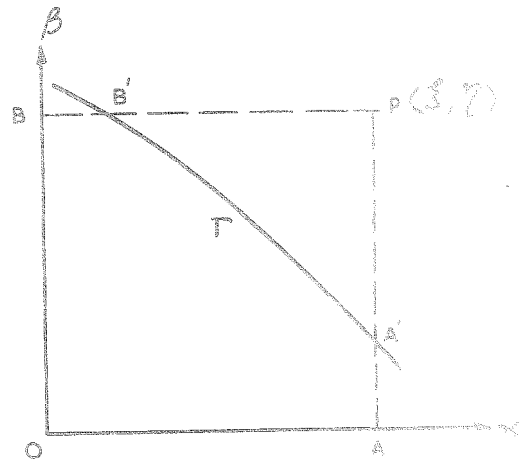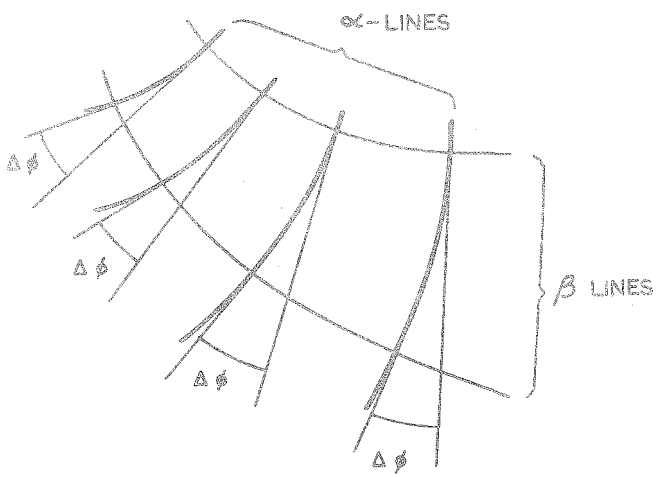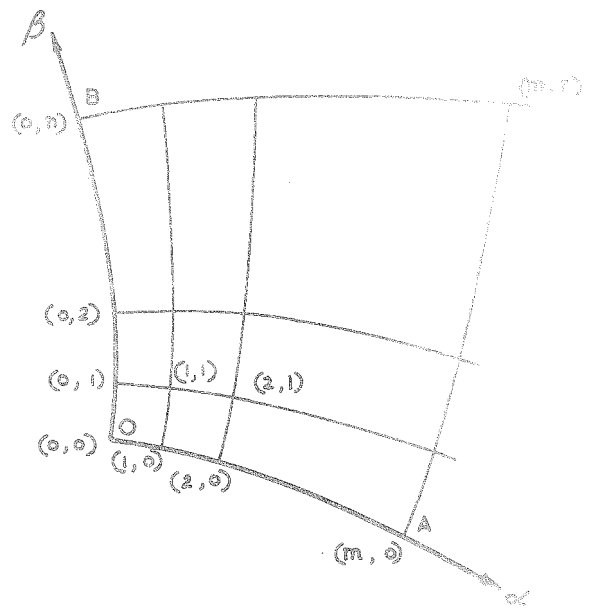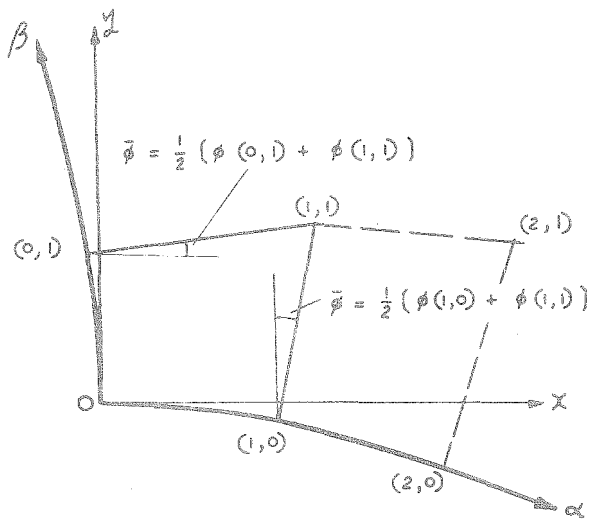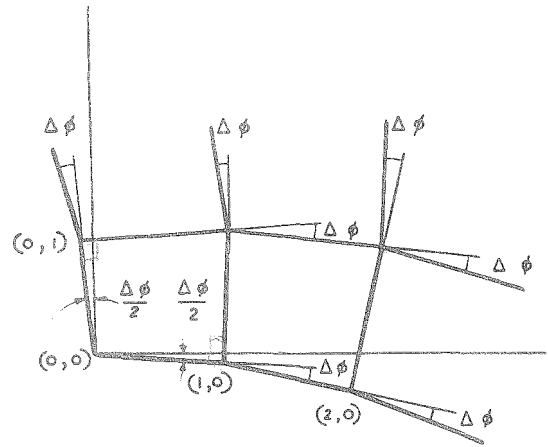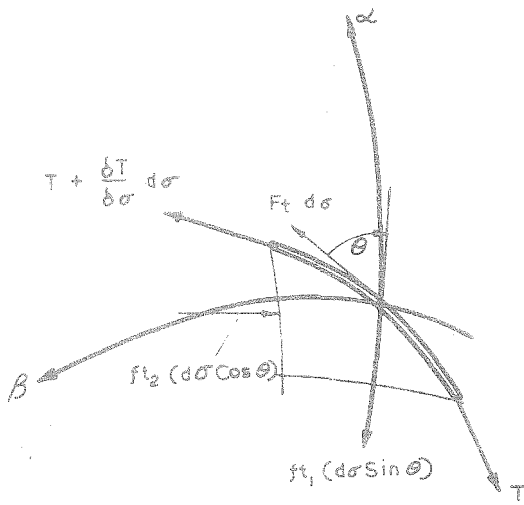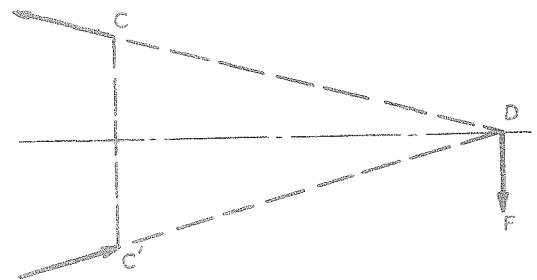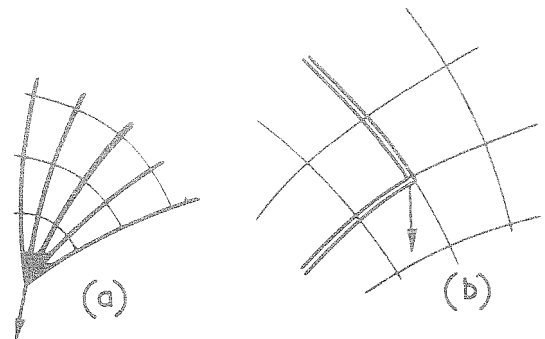
FIG. 11.
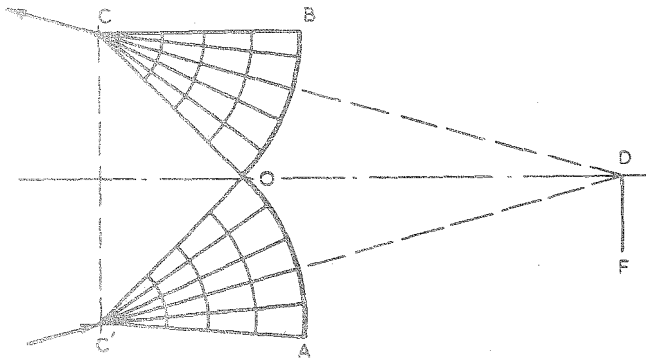
FIG. 12.
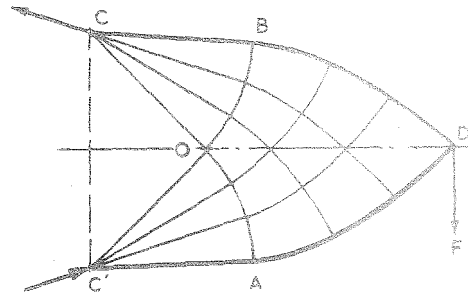
FIG. 13.
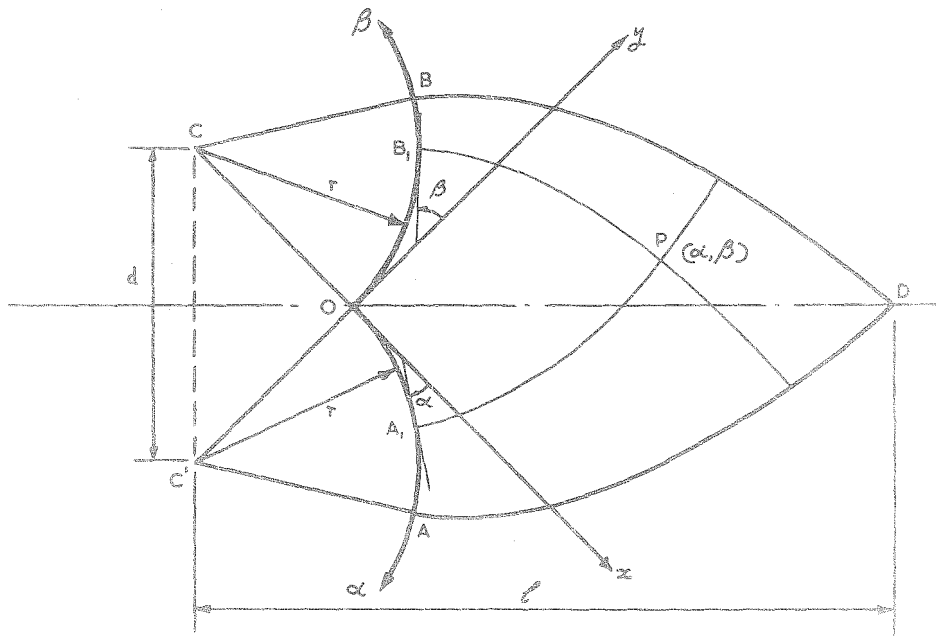
FIG 14
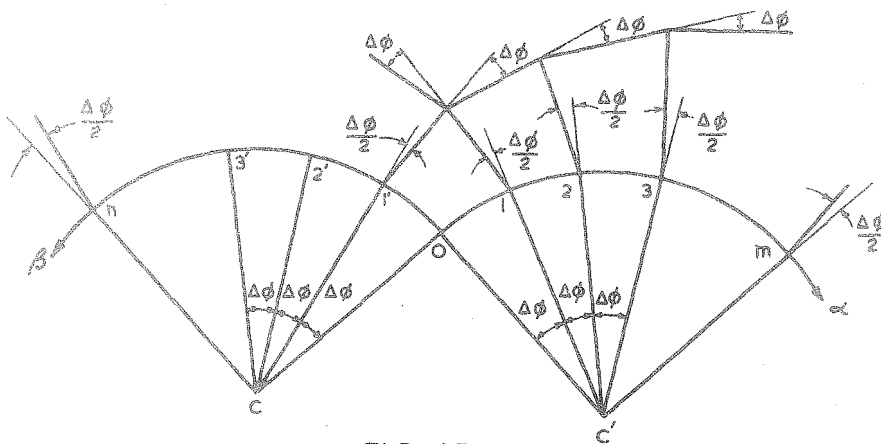
FIG. 15.
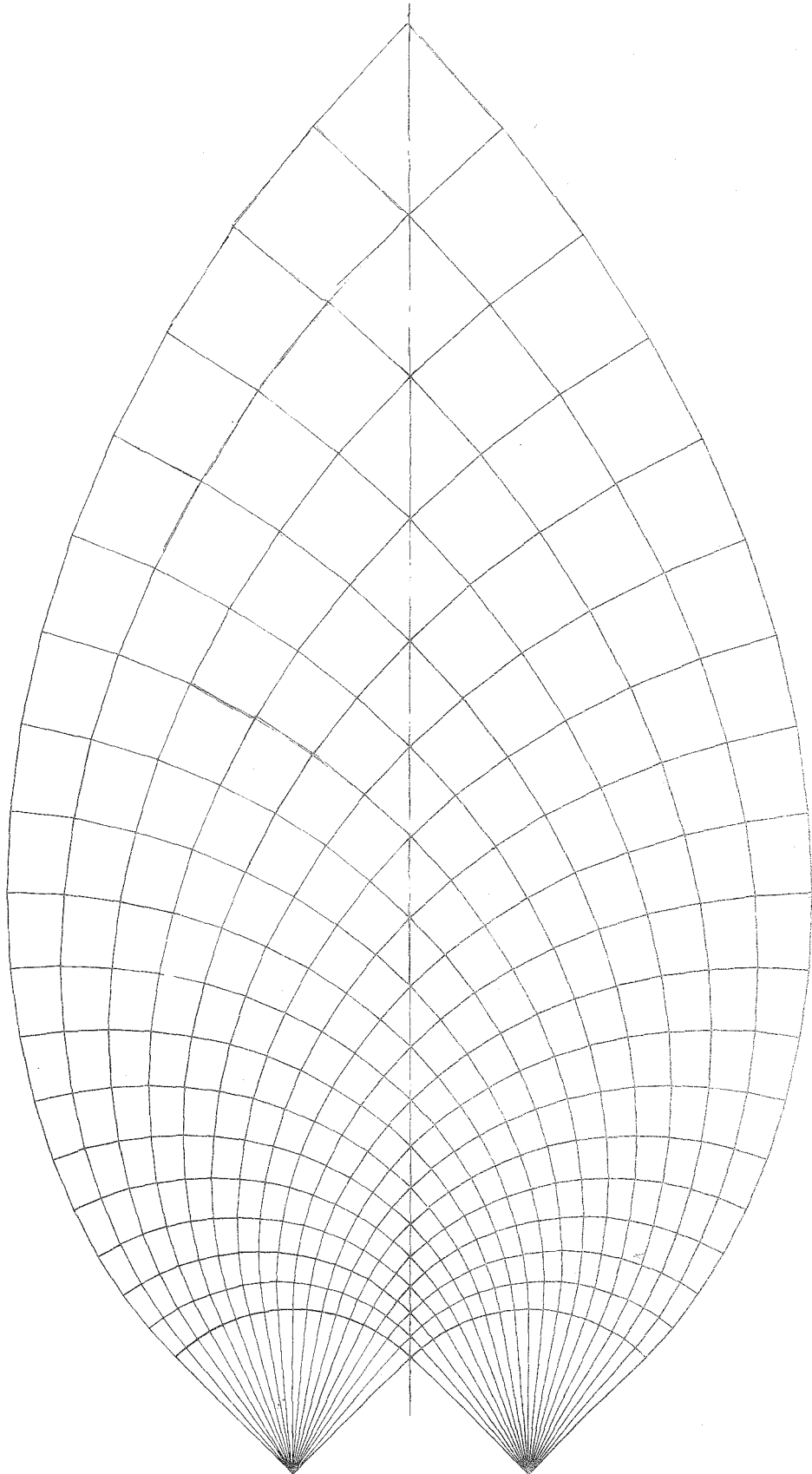
FIG. 16
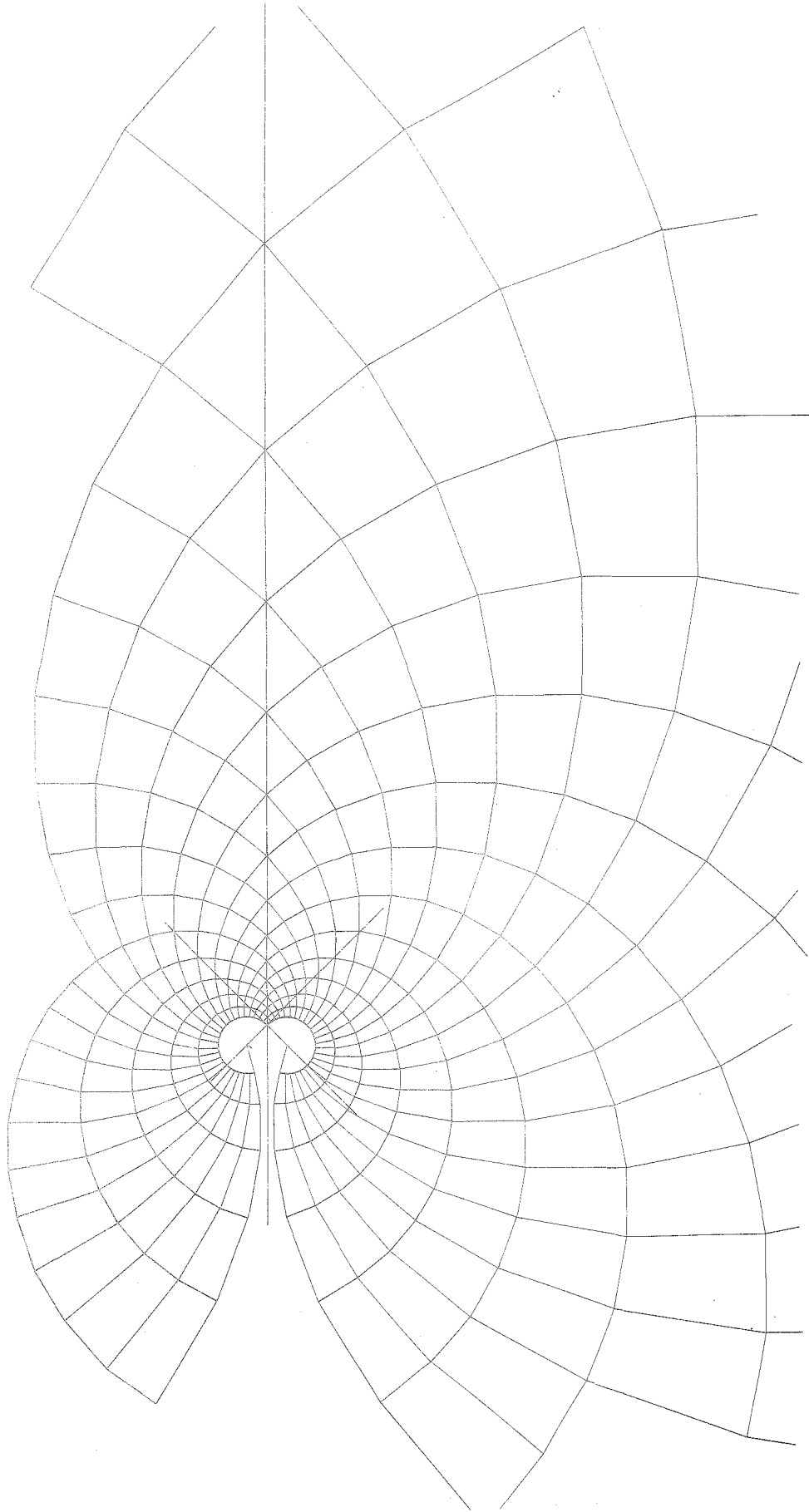
FIG. 17
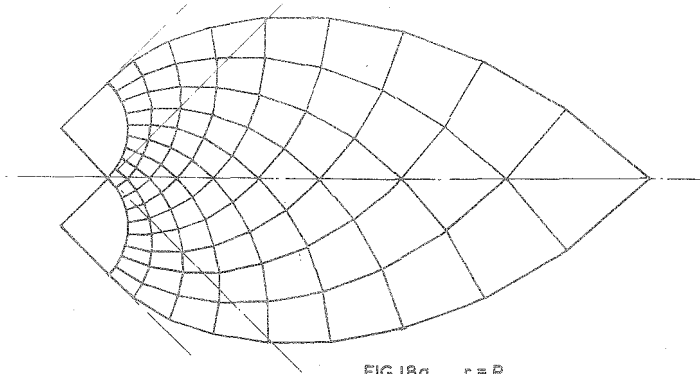
FIG. 18a.   r = R
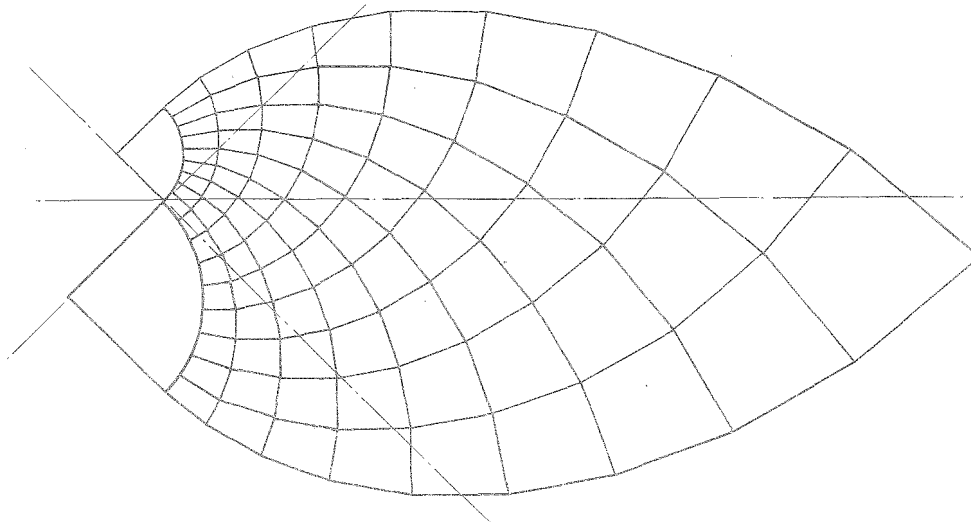
FIG. 18 b. $\frac{r}{R} = \frac{1}{2}$
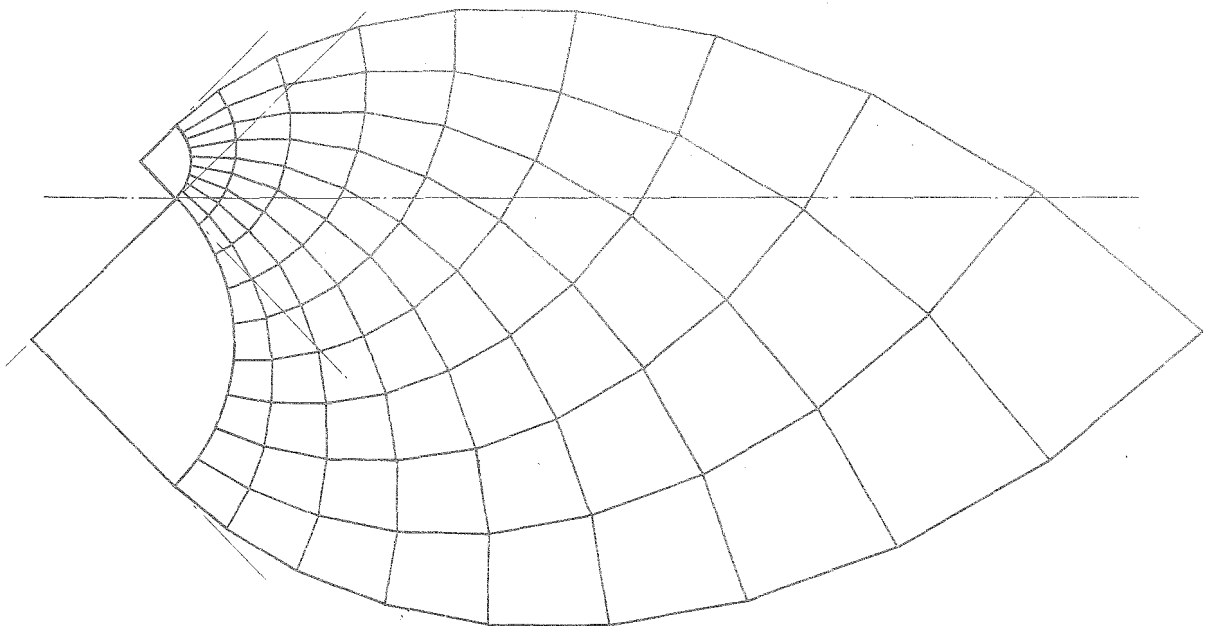
FIG. 18 c. $\frac{r}{R} = \frac{1}{4}$
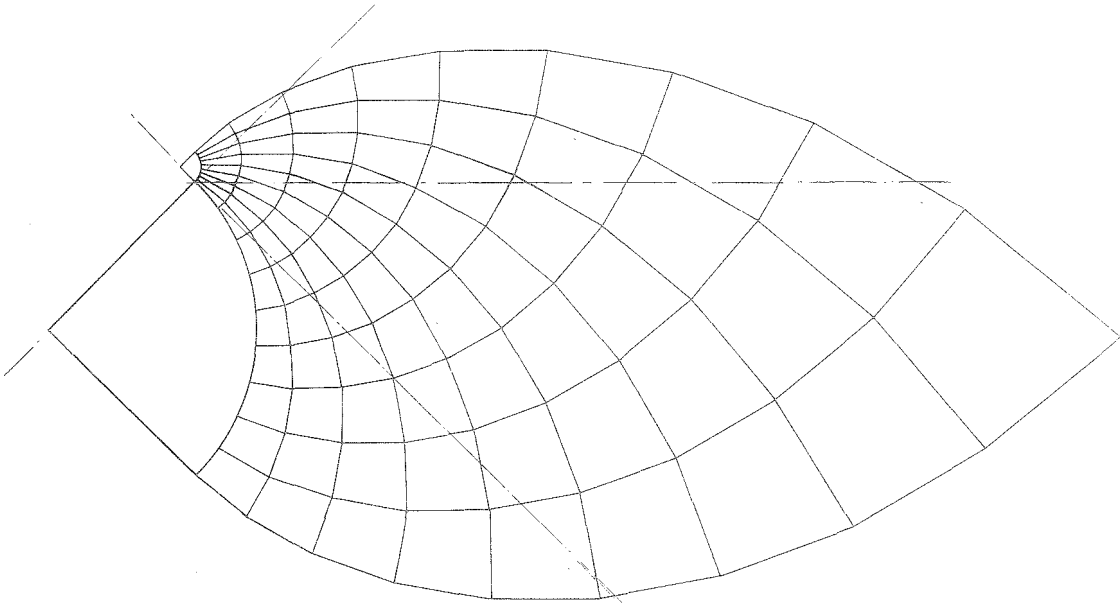
FIG. 18

FIG. 18 d. $\frac{r}{R} = \frac{1}{10}$
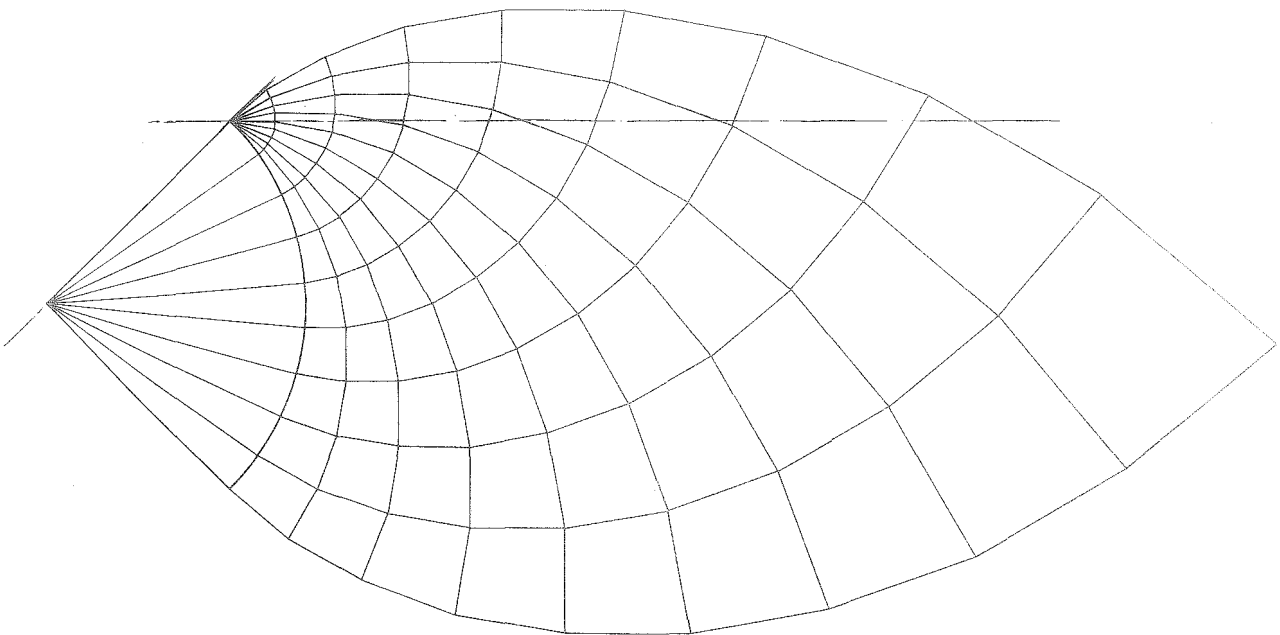
FIG.18 e. $\frac{r}{R} = 0$

FIG. 18
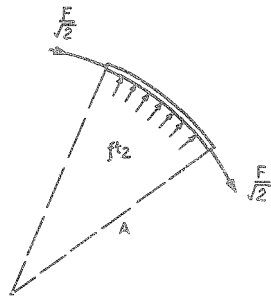
FIG.19.
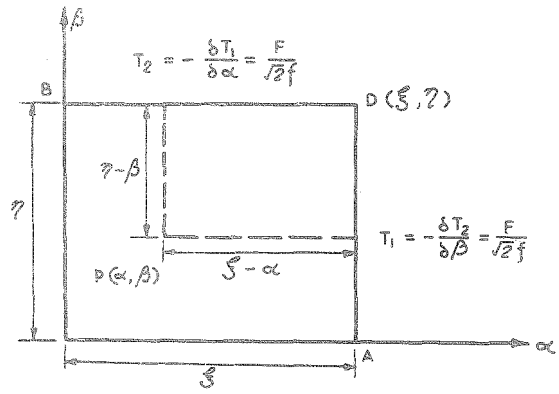
FIG. 20.
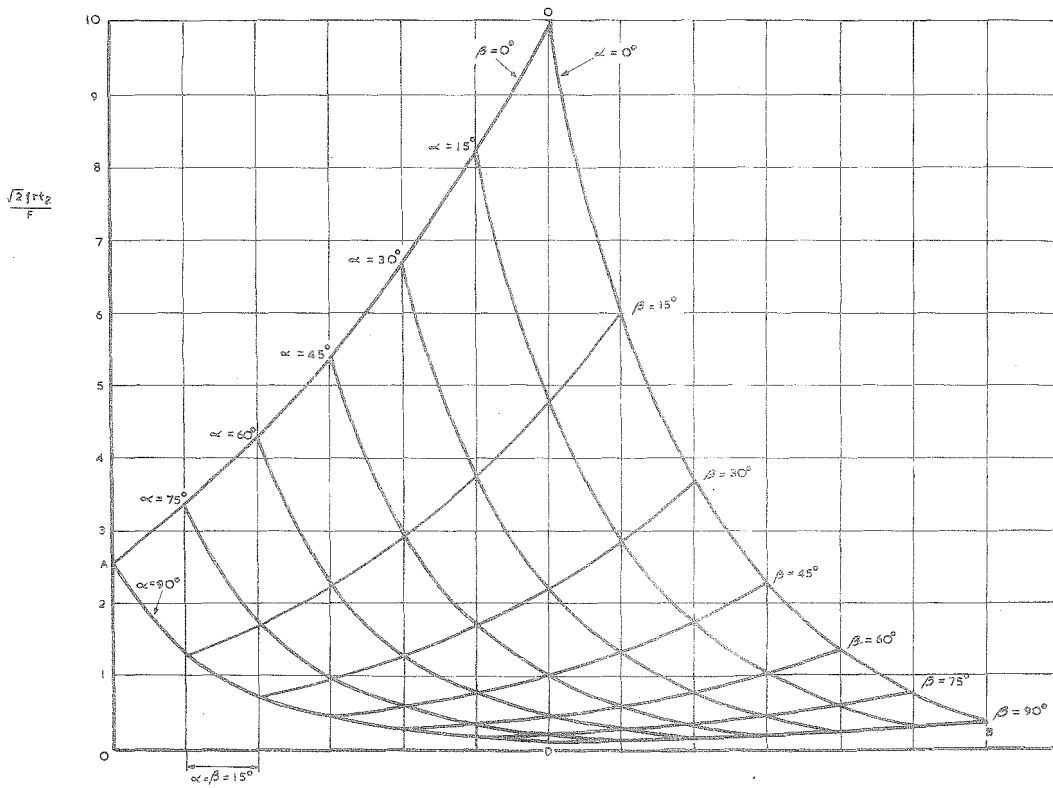
FIG. 21. EQUIVALENT THICKNESS OF SHEET IN A FIELD
DEFINED BY TWO EQUAL 90° FANS

(a) AT POINT D   (b) JOINTS OUTSIDE OB   (c) JOINTS ON OB

FIG. 22.

FIG. 24.
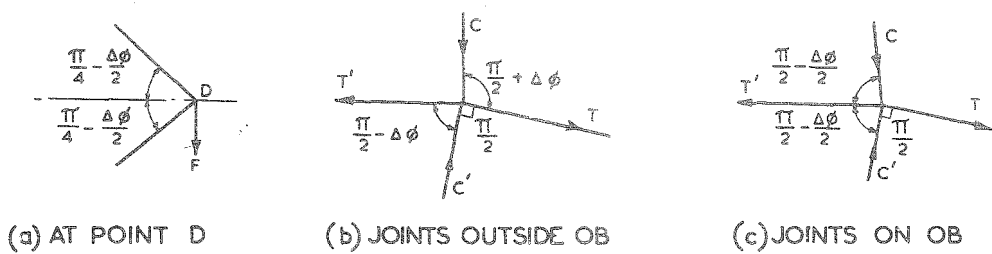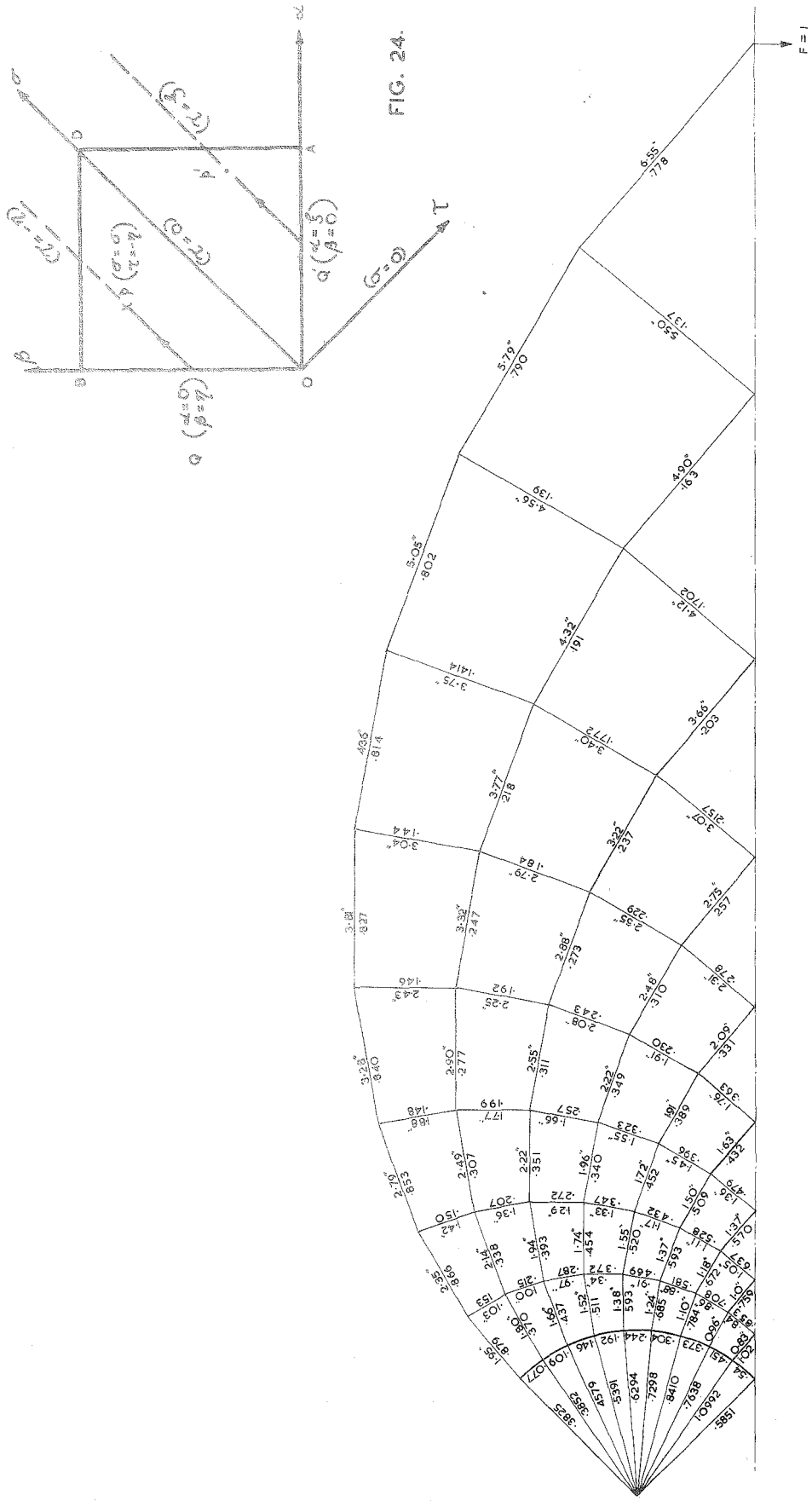
FIG. 23. LOADS IN THE MEMBERS OF THE MICHEL CANTILEVER
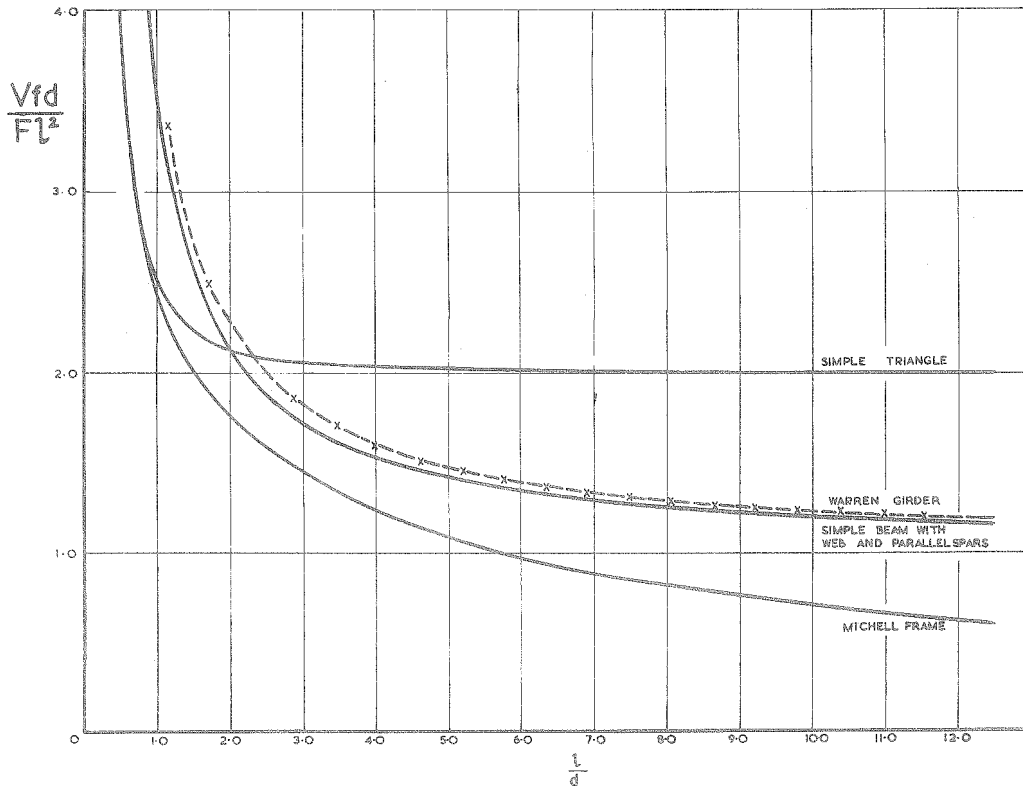DUE TO A UNIT LOAD AT THE TIP
(RADIUS OF FAN = 4.0 INCHES)

FIG. 25. COMPARISON OF THE VOLUME OF VARIOUS
CANTILEVER STRUCTURES

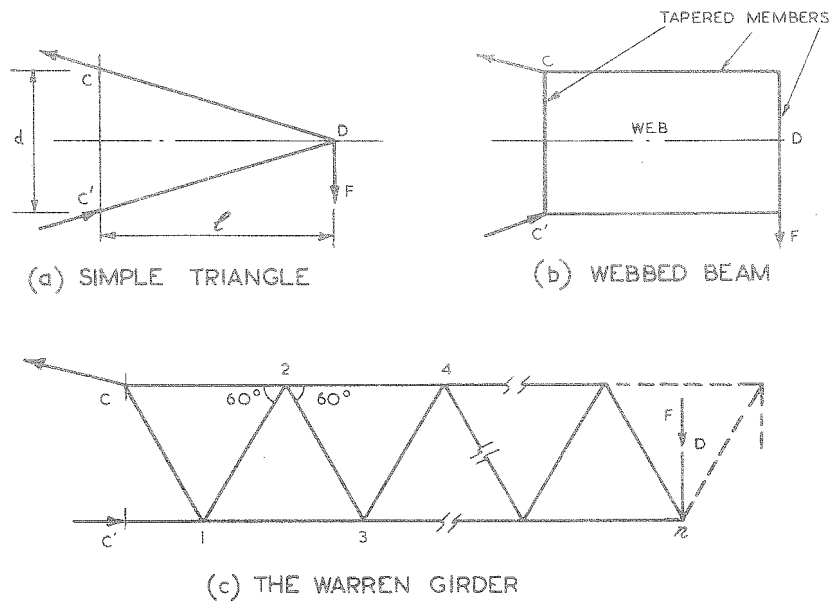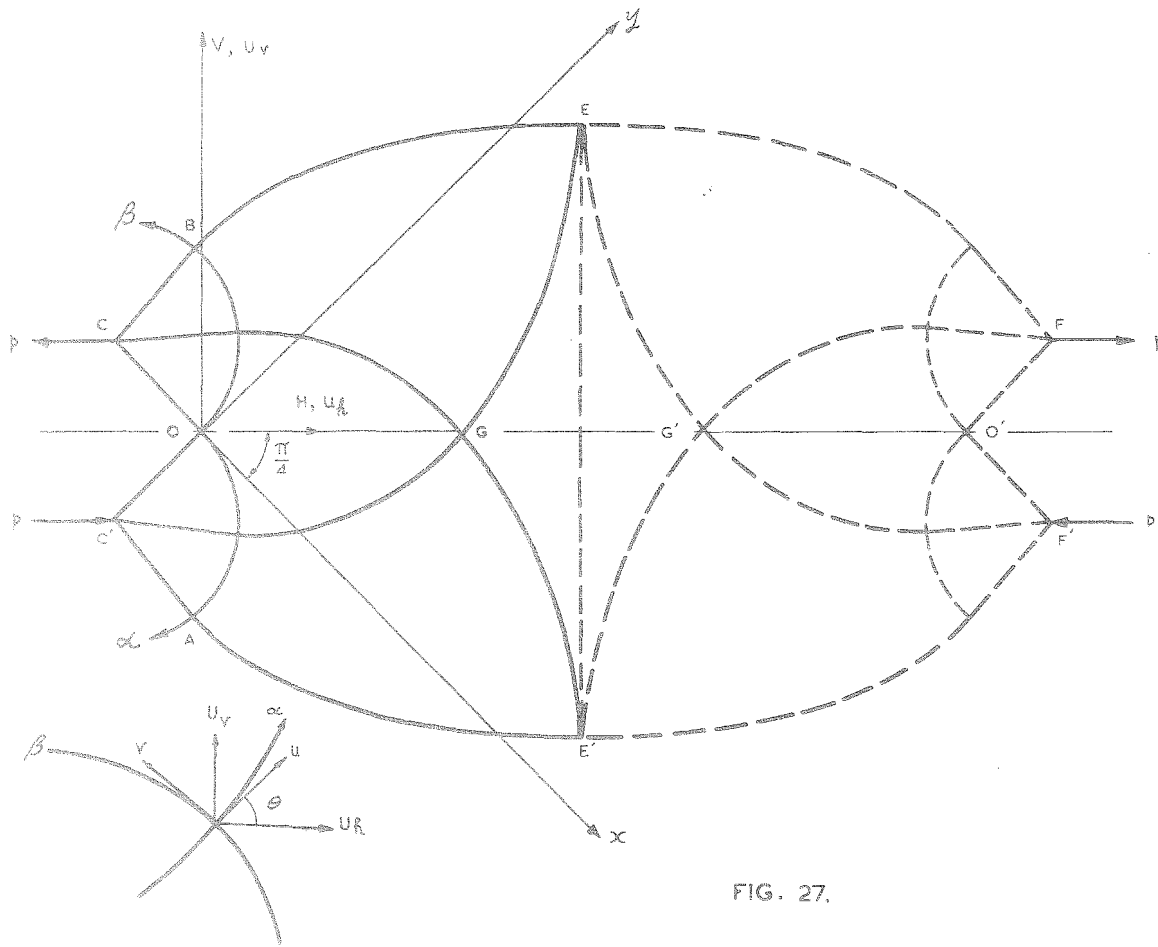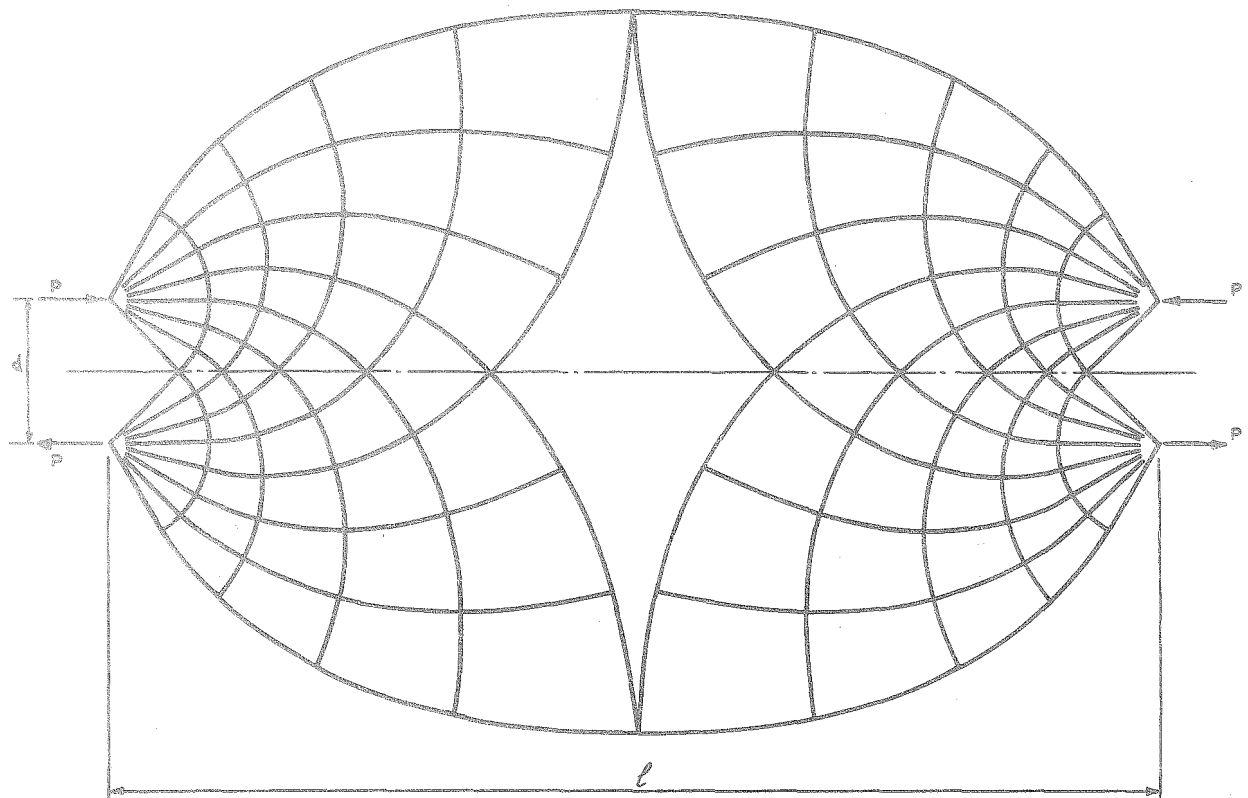(a) SIMPLE TRIANGLE   (b) WEBBED BEAM

(c) THE WARREN GIRDER

FIG. 26.

FIG. 27.

FIG. 28. OPTIMUM STRUCTURE FOR PURE BENDING MOMENT

FIG. 29. COMPARISON OF THE WEIGHT OF VARIOUS BEAMS
UNDER PURE BENDING

FIG. 30